Amyloid β-peptide-induced progressive neurodegeneration in an APP-transgenic mouse model for Alzheimer's disease

Dissertation/
Doctoral Thesis

zur/for

Erlangung des Doktorgrades (Dr. rer. nat.)/
PhD degree in Natural Science

der/from the

Mathematisch-Naturwissenschaftlichen Fakultät/
Faculty of Mathematics and Natural Science

der/from the

Rheinischen Friedrich-Wilhelms-Universität Bonn/
Rheinischen Friedrich-Wilhelms-University of Bonn

Estibaliz Capetillo Gonzalez de Zarate

aus/from

Getxo, Spanien/Spain

Bonn 2006

Anfertigung mit Genehmigung der Mathematisch-Naturwissenschaftlichen Fakultät der Rheinischen Friedrich-Wilhelms-Universität Bonn.

1. Referent: **PD. Dr. D. R. Thal**
2. Referent: **Professor Dr. W. Kolanus**

Tag der Promotion/Day of the defence: **October 27, 2006**

Thesis electronically published at: **http://hss.ulb.uni-bonn.de/diss_online**

Thesis work: Faculty of Medicine-Department of Neuropathology
Universitätsklinikum Bonn
Sigmund Freud Strasse 25
D-53105 Bonn, Germany

Thesis defence: Faculty of Mathematics and Natural Sciences
Rheinische Friedrich Wilhelms Universität Bonn
Wegeler Strasse 10
D-53115 Bonn, Germany

Author: Estibaliz Capetillo Gonzalez de Zarate
Faculty of Medicine-Department of Neuropathology
Universitätsklinikum Bonn
Sigmund Freud Strasse 25
D-53105 Bonn, Germany

Telephone: 0228 287-1-6394
Fax: 0228 287-1-4331
E-mail: ecapetil@uni-bonn.de

Degree in Biology
Master in Human Neurobiology

Supervisor: PD. Dr. med. Dietmar R. Thal
Faculty of Medicine- Department of Neuropathology
Universitätsklinikum Bonn
Sigmund Freud Strasse 25
D-53105 Bonn

Telephone: 0228 287-1-5775
E-mail: Dietmar.Thal@uni-bonn.de

Defence committee: PD. Dr. med. D. R. Thal

Prof. Dr. rer. nat. W. Kolanus

Prof. Dr. rer. nat. K. Willecke

PD. Dr. rer. nat. G. van Echten-Deckert

CONTENTS

ABSTRACT

The amyloid β-protein (Aβ) is the main component of Alzheimer's disease (AD)-related senile plaques. In the human brain Aβ-deposition occurs in a hierarchical sequence in which different areas of the brain become involved. It is not clear whether this sequence shows the time course of Aβ-deposition or just different pathology in different individuals. Although Aβ is associated with the development of AD it has not been shown which forms of Aβ induce neurodegeneration in vivo, which types of neurons are vulnerable and whether Aβ-induced neurodegeneration increases with the progression of Aβ-pathology. To address these questions, DiI-crystals were implanted into the left frontocentral cortex of APP23 transgenic mice overexpressing mutant human APP and of wild-type littermates. In parallel, immunohistochemistry for Aβ-plaque detection was performed in 3-, 5-, 11-, 15- and 25-month-old APP23 mice and wild-type littermates. Traced commissural neurons in layer III of the right frontocentral cortex were quantified in 3-, 5-, 11-, and 15-month-old mice. Three different types of commissural neurons were traced. At 3 months of age no differences in the number of labeled commissural neurons were seen in APP23 mice compared to wild-type mice. A selective reduction of the heavily ramified type of neurons was observed in APP23 mice compared to wild-type animals at 5, 11, and 15 months of age, starting with the deposition of Aβ-plaques occurred in the frontocentral cortex at 5 months of age. The other two types of commissural neurons did not show alterations in 5- and 11-month animals. At 15 months of age, the number of traced sparsely ramified pyramidal neurons was reduced in addition to that of the heavily ramified neurons in APP23 mice compared with wild-type mice. At this point in time Aβ-deposits were seen in the neo- and allocortex as well as in the basal ganglia and the thalamus. At 25 months of age Aβ-deposits were also seen at the brainstem. In summary, the results show that 1) Aβ-deposition in APP23 mice follows a similar sequence as in human brain, in which the different areas become step-by-step involved in β-amyloidosis, 2) this step-

by-step regional involvement represents the time course of Aβ-deposition in the brain, and 3) Aβ, thereby, induces progressive degeneration of distinct types of commissural neurons. Degeneration of the most vulnerable neurons starts in parallel with the occurrence of the first fibrillar Aβ deposits in the neocortex. The selective vulnerability of different types of neurons to Aβ is presumably related to the complexity of their dendritic morphology. In so doing, these results support Aβ to be the major therapeutic target for AD treatment in pre-clinical as well as in late stages of the disease.

ABBREVIATIONS

2D	Two dimensions
3D	Three dimensions
Aβ	Amyloid β-protein
ABC complex	Avidin biotin peroxidase complex
ANOVA	Analysis of variance
ADDL	Aβ-derived diffusible ligand
AD	Alzheimer's disease
AICD	APP intracellular domain
APH	Anterior pharynx defective protein
ApoE	Apolipoprotein E
APP	Amyloid precursor protein
APPS	Soluble APP N-terminal fragment
BACE	β-secretase cleavage enzyme
BDA	Biotinylated dextrane amine
CAA	Cerebral amyloid angiopathy
cDNA	Complementary deoxyribonucleic acid
Cg	Cingulate cortex
CTF	C-terminal fragment
DAB	3, 3-diaminobenzidine

ddH_20	Double destilled hydrogen oxide
DiI	1,1'-dioctadecyl-3,3,3',3'-tetramethylindolcarbocyanine perclorate
dNTP	Deoxynucleotides
EDTA	Ethylenediaminetetraacetic acid
ELISA	Enzyme linked inmunoabsorvent assay
EtBr	Ethidium Bromide
F	Phenylalanine
GAP43	Growth association protein 43
H_2O_2	Hydrogen peroxide
hAPP	Human amyloid precursor protein
HCl	Hydrogen chloride
HP	Hippocampus
hPrP	Hamster prion protein promoter
I	Isoleucine
K	Lysine
KDa	KiloDalton
KI	Knock-in
L	Leucine
LTP	Long term potentiation
M (amino acid)	Methionine

M (concentration)	molar
M1	Primary motor cortex
M2	Secondary motor cortex
$MgCl_2$	Magnesium chloride
mRNA	Messenger ribonucleic acid
N	Asparagine
n	Number of animals
Na_2EDTA	Disodium ethylenediaminetetraacetic acid
Na_2HPO_4	Disodium hydrogen phosphate
NaCl	Sodium Chloride
NaH_2PO_4	Sodium dihydrogen phosphate
NaOH	Sodium hydroxide
NFP	Neurofibrillary pathology
NFT	Neurofibrillary tangles
NMDA	N-methyl-D-aspartic acid
P	Proline
p3	Peptide produce by sequential cleavage of APP by α- and β-secretases
PBS	Phosphate buffer solution
PCR	Polymerase chain reaction
PHF	Paired helical filament

pHMG	p-Hydroxymethyl CoA reductase
PDGF-β	Platelet derived growth factor-β
PCR	Polymerase Chain Reaction
PEN-2	Presenilin enhancer protein-2
PFA	Para formaldehyde
PS	Presenilin
S1	Primary somatosensory cortex
SDS	Sodium dodecyl sulfate
TAE	Tris acetate EDTA
TBS	Tris buffer solution
Thy	Thymocyte
Tris HCl	Tris hydrochloride
UV	Ultraviolet
V	Valine

1. INTRODUCTION

In 1907 the German psychiatrist and neuropathologist Dr. Alois Alzheimer described changes in the brain of a 55-year-old woman dying after a 4-year history of progressive dementia (Alzheimer, 1907). The leading symptoms were: progressive memory impairment, disordered cognitive function, altered behavior including paranoia, delusions, loss of social appropriateness, and a progressive decline in language function. In his report, Alzheimer demonstrated neurofibrillary tangles using the Bielschowsky silver impregnation method and he also observed cortical senile plaques (Alzheimer, 1907), already described 15 years earlier by Blocq and Marinesco (Blocq and Marinesco, 1892). This was the first reported case of a disease which is today known as Alzheimer's disease (AD).

1.1. Alzheimer type dementia

AD is a neurodegenerative disorder, which is clinically characterized by progressive cognitive decline finally leading to the full-blown picture of dementia (Duyckaerts and Dickson, 2003). AD is the most common cause of dementia and represents 50-70% of all dementias (Lamy et al., 1989; Ferri et al., 2005).

The prevalence of dementia and AD, which is the number of cases in a population at given point in time, increases when comparing this parameter in different age groups with advancing age. Between 65- to 69-year-old individuals the prevalence of dementia is approximately 1%. It duplicates with each subsequent 5-year interval. Over 85 years of age, the prevalence varies between 20%-50% (Lamy et al., 1989). The incidence, which is the number of newly diagnosed cases in a given time interval, also increases dramatically with advancing age when comparing this parameter in different age groups.

From 70 to 80 years of age, the number of new cases increases more than 1%. Above 80 years of age, the number increases to 2% (Knopman, 2003).

Cognitive deficits in AD are characterized by deficits in learning and retaining new information (Storandt et al., 1984; Knopman and Ryberg, 1989; Welsh et al., 1991; Petersen et al., 1994; Grober and Kawas, 1997). Problems in word finding and loss of conversational skills are the most relevant language deficits related to the disease (Knopman, 2003). The patients show deficits in spatial ability, orientation and in reasoning or handling complex tasks, alterations in mood or behavior, and in basic activities of daily living that characterize the disease (Knopman, 2003).

The major risk factors for AD are advanced age, a family history of dementia and presence of an apolipoprotein E (ApoE) ε4 allele (Heston et al., 1981; Corder et al., 1993; Mayeux et al., 1995; Lautenschlager et al., 1996). Low educational achievement increases the risk of developing dementia by 2- to 3- fold (Zhang et al., 1990; Friedland, 1993; Katzman, 1993; Stern et al., 1994; Cobb et al., 1995; Ott et al., 1995; Stern et al., 1995; Callahan et al., 1996). Cardiovascular disease (Elias et al., 1993; Hofman et al., 1997; Clarke et al., 1998) and elevated serum homocysteine has also been associated with dementia although the biological link between homocysteine and AD has not been clarified so far (Clarke et al., 1998; McCaddon et al., 1998; Kalmijn et al., 1999; Seshadri et al., 2002). Possible protective factors are active life style, low cholesterol levels, education, and the use of estrogen and non-steroidal anti-inflammatory drugs (Knopman, 2003).

AD is morphologically characterized by cerebral atrophy, i.e. loss of brain weight and volume, thickness and length of the cortical ribbon and ventricular dilatation (Duyckaerts and Dickson, 2003). The degree of cortical atrophy varies and seems to correlate with cognitive decline (Mouton et al., 1998).

Microscopically, senile plaques, intracellular neurofibrillary tangles (NFT) and vascular amyloid deposits are the hallmark of AD (Alzheimer, 1907; Masters et al., 1985a; Braak and Braak, 1991b; Dickson, 1997; Esiri et al., 1997; Duyckaerts and Dickson, 2003). In addition, neuronal and

synaptic loss is also associated with AD (Terry et al., 1981; Braak and Braak, 1991b; Duyckaerts and Dickson, 2003). An early morphological correlative for neuronal loss is corpus callosum atrophy which can be detected in living patients by imaging techniques (Weis et al., 1991; Yamauchi et al., 1993; Hampel et al., 1998).

1.2. Amyloid-β protein deposition

Amyloid deposits consist of extracellular insoluble fibrillar proteins or peptides with a high content of β-pleated sheet secondary structure and show a characteristic red-green birefringence in Congo red-stained sections (Virchow, 1854, 1855). The aggregated protein in the senile plaques and vascular amyloid deposits in brain of AD-patients is the amyloid β-protein (Aβ) (Glenner and Wong, 1984; Masters et al., 1985b).

1.2.1. Aβ production and degradation

Aβ is a 40-42 amino acid peptide of 4 KDa. It is derived from the amyloid precursor protein (APP) by sequential proteolytic cleavage (Kang et al., 1987; Haass et al., 1992). APP is an internal type I membrane glycoprotein. It has a large amino terminal extracellular/luminar domain (ectomain) and a short cytoplasmic tail. APP is expressed as three alternatively spliced isoforms: APP695 (neuronal form), and APP770/751 isoforms (peripheral and glial isoforms) (Kang et al., 1987; Dyrks et al., 1988; Kitaguchi et al., 1988; Ponte et al., 1988; Tanzi et al., 1988).

APP can be metabolized by two pathways (fig. 1) (Haass et al., 1992): The non-amyloidogenic pathway and the amyloidogenic pathway. The non-amyloidogenic pathway is characterized by α-secretase cleavage of APP within the Aβ domain (between residues K16 and L17 of Aβ). This cleavage results in the release of a large soluble N-terminal fragment (APPSα) into the lumen of the

organelles or into the extracellular space and the retention of α-C-terminal fragment (α-CTF) in the membrane. Subsequently, γ-secretase complex (a multimeric protein complex that includes presenilin (PS)-1 or PS2, nicastrin, anterior pharynx defective protein (APH)-1 and presenilin enhancer protein (PEN)-2) cleavages α-CTF within the transmembrane domain generating an N-terminal truncated Aβ (p3) and APP intracellular domain (AICD) (Cao and Sudhof, 2001; Cupers et al., 2001; Kimberly et al., 2001). On the other hand, the amyloidogenic pathway generates a soluble N-terminal fragment (APPSβ) and a C-terminal fragment (β-CTF) in the membrane by β-secretase cleavage (between residues M671 and N672 of APP) generating the N-terminus of Aβ (Vassar et al., 1999). Subsequent cleavage by γ-secretase complex produces Aβ and AICD (Haass et al., 1992).

In healthy brains secreted Aβ is catabolized by astrocytes (Koistinaho et al., 2004). Apparently, Aβ binds to ApoE and such Aβ-ApoE complexes are taken up by astrocytes (Koistinaho et al., 2004) and subsequently become enzymatically degraded by neprilysin, insulin degrading enzyme and/or endothelin-degrading enzyme (Iwata et al., 2000; Eckman et al., 2001; Miller et al., 2003). Since ApoE is also involved in the formation of newly-form plaques (Thal et al., 2005) other clearance mechanisms have been investigated. Drainage of extracellular Aβ via perivascular channels has also been shown to be a significant mechanism for clearing Aβ from the brain, especially for ApoE-Aβ complexes (Weller et al., 1998; Thal et al., 2006b).

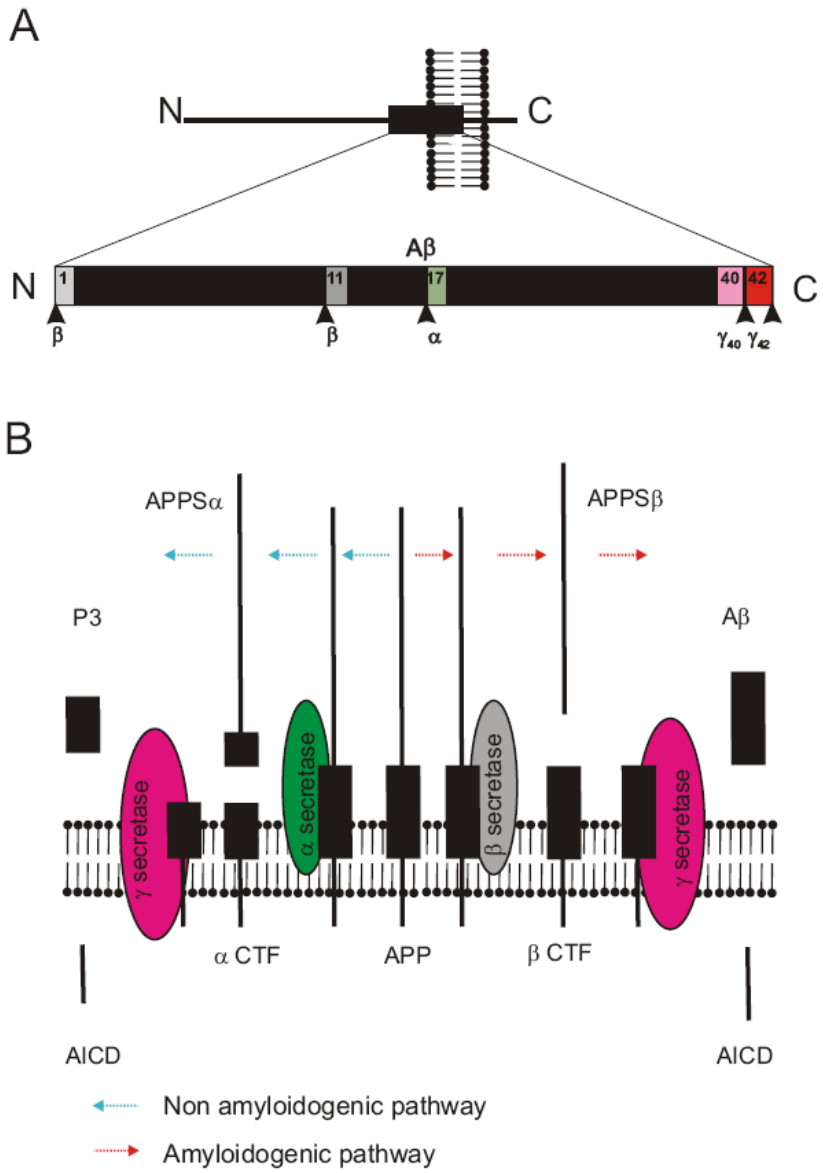

Figure 1: APP metabolism. **A**: Schematic representation of APP within the membrane. Aβ peptide location within APP is enlarged. α-, β- and γ-secretase cleavage sites are indicated. There is a minor cleavage site of β-secretase at 11 amino acid (schematic representation modified from (Thal et al., 2006a) **B**: Amyloidogenic and non-amyloidogenic processing of Aβ. The non-amyloidogenic processing of APP by α- and γ-cleavage results in the generation of APPSα, p3 and AICD. The amyloidogenic processing of APP by β- and γ-secretases cleavage produces APPSβ, Aβ and AICD (schematic representation modified from (Vetrivel and Thinakaran, 2006).

1.2.2. Pathological accumulation of Aβ

Under pathological conditions Aβ accumulates in the brain. Monomeric Aβ aggregates to oligomers, protofibrils and finally to amyloid fibrils. A prerequisite for Aβ aggregation is the increase of Aβ concentration (Masters and Beyreuther, 2003). This increase may be due to increase of Aβ production or due to reduction of Aβ clearance. In familiar AD, mutations in the APP gene or in the PS1/PS2 genes lead to an increased production of Aβ (Hardy, 1997; Bertram and Tanzi, 2003; Masters and Beyreuther, 2003). However, in sporadic AD no increase in Aβ-production has been detected but a reduction of Aβ degradation (Schenk et al., 1999; Iwata et al., 2000; Masters and Beyreuther, 2003; Miller et al., 2003; Koistinaho et al., 2004).

Mutations that modify the amino acid sequence of the Aβ-protein modulate its tendency to form insoluble protofibrils and fibrils (Nilsberth et al., 2001; Morimoto et al., 2004). Both, intracellular and extracellular aggregates of Aβ seem to be neurotoxic (Vidal et al., 1999; Wirths et al., 2001; Takahashi et al., 2004; Kokubo et al., 2005a; McGowan et al., 2005; Lord et al., 2006) but not monomeric Aβ (Pike et al., 1991). However, consecutive aggregation of Aβ monomers leads to soluble Aβ oligomers called Aβ derived diffusible ligands (ADDLs). Intracellular (Takahashi et al., 2004) and extracellular ADDLs are neurotoxic (Kayed et al., 2003; Kim et al., 2003; Lacor et al., 2004). A recent study in Tg2576 mice shows that extracellular accumulation of soluble 56KDa $A\beta_{1-42}$ assemblies (Aβ*56) can be responsible for the memory deficits prior to amyloid deposition in these mice (Lesne et al., 2006).

Aβ fibrils, derived from ADDLs appear to induce degeneration of neurites and neurons and result in the development of senile plaques (Calhoun et al., 1998; Schmitz et al., 2004; Tsai et al., 2004). Although recent publications indicate an involvement of ADDLs in early Aβ-induced

neurotoxicity, further studies are necessary to clarify the possible role of ADDLs in early degeneration of neurons and to identify which neuronal compartments may be critical for Aβ-induced neurotoxicity.

1.2.3. Amyloid deposits

Senile plaques differ in their composition, both in terms of the type of Aβ peptides deposited and in terms of other proteins additionally found in Aβ-plaques (Thal et al., 2006a). The two major forms of monomeric Aβ are: $A\beta_{1-40}$ and $A\beta_{1-42}$ (Glenner and Wong, 1984; Masters et al., 1985b; Iwatsubo et al., 1994) representing a 40 and 42 amino acid peptide, respectively. In addition to $A\beta_{1-40}$ and $A\beta_{1-42}$, N-terminal truncated forms of Aβ were also seen in Aβ-plaques. The most common forms of N-terminal truncated Aβ peptides are: $A\beta_{3-40/42}$, $A\beta_{11-40/42}$ and p3 ($A\beta_{17-40-42}$) (Saido et al., 1995; Saido et al., 1996). Other proteins occurring in senile plaques are the ApoE, α_2-macroglobulin, interleukin 1α, interleukin 6, components of the complement system, α_2-macroglobulin receptor/low density lipoprotein receptor-related protein and collageneous Alzheimer amyloid component/collagen XXV (Griffin et al., 1989; McGeer et al., 1989; Namba et al., 1991; Strauss et al., 1992; Rebeck et al., 1993; Thal et al., 1997; Hashimoto et al., 2002).

1.2.3.1.Classification of senile plaques

According to the varying protein composition and the morphology of the plaques, different types can be distinguished in the human brain (Table 1) (Duyckaerts and Dickson, 2003; Thal et al., 2006a).

Table 1. Summary of different types of Aβ-plaques (from (Thal et al., 2006a).

Plaque type	Morphological determination
1. Diffuse plaque	a) Sharply delineated Aβ42-positive diffuse plaque not detectable with antibodies raised against N-terminal epitopes of Aβ. These plaques also exhibit apoE very often. b) Fleecy amyloid: III-bordered clouds of Aβ42-positive diffuse plaque not detectable with antibodies raised against N-terminal epitopes of Aβ. These plaques also exhibit apoE very often. c) Sharply delineated ApoE-negative diffuse plaques exhibiting N-terminal epitopes of Aβ. d) Diffuse plaque containing apoE and exhibiting N-terminal epitopes of Aβ. e) Diffuse "APP-type" neuritic plaque = Diffuse plaque with APP-positive dystrophic neurites f) Diffuse "PHF-type" neuritic plaque = Diffuse plaque with neurofibrillary material in dystrophic neurites. g) Diffuse "a-synuclein-type" neuritic plaques = Diffuse neuritic plaques containing a-synuclein-positive dystrophic neurites. This type of diffuse plaque is restricted to AD cases with combined Parkinson's disease. (=Lewy-Plaque).
2. Subpial band-like Aβ	Sharply-delineated, evenly distributed band-like Aβ within the subpial portion of the molecular layer of the temporal and entorhinal cortex.
3. Lake-like amyloid	Sharply delineated, evenly distributed Aβ-deposits within the parvopyramidal layer of the presubicular region; containing neuronal perikarya of normal appearance.
4. Cored plaque (=Classical Plaque)	a) Sharply delineated Aβ-deposits with an amyloid core in the center surrounded by a corona of diffuse Aβ-deposits. Between the core and the corona is a small gap without Aβ. b) Cored "APP-type" neuritic plaque = Cored plaque with APP-positive dystrophic neurites. c) Cored "PHF-type" neuritic plaque = Cored plaque with neurofibrillary material in dystrophic neurites. d) Cored "α-synuclein-type" neuritic plaques = Cored neuritic plaques containing α-synuclein-positive dystrophic neurites. This type of cored plaque is restricted to AD cases with combined Parkinson's disease.
5. Core-only plaque (=burned-out plaque or compact plaque)	Pure, sharply delineated amyloid cores without associated diffuse Aβ-deposits.
6. White matter plaque	a) Diffuse type: Sharply delineated, evenly distributed Aβ-deposits within the white matter. b) Globular type: Sharply delineated Aβ-deposits in the white matter containing globular aggregates of Aβ.
7. Cotton wool plaque	Sharply delineated evenly distributed Aβ-deposits in roundish, cotton wool-like amyloid plaques without amyloid core and without neuritic changes. Predominance of this plaque type is a characteristic feature for a subset of familial AD cases harbouring a presenilin 1 mutation.

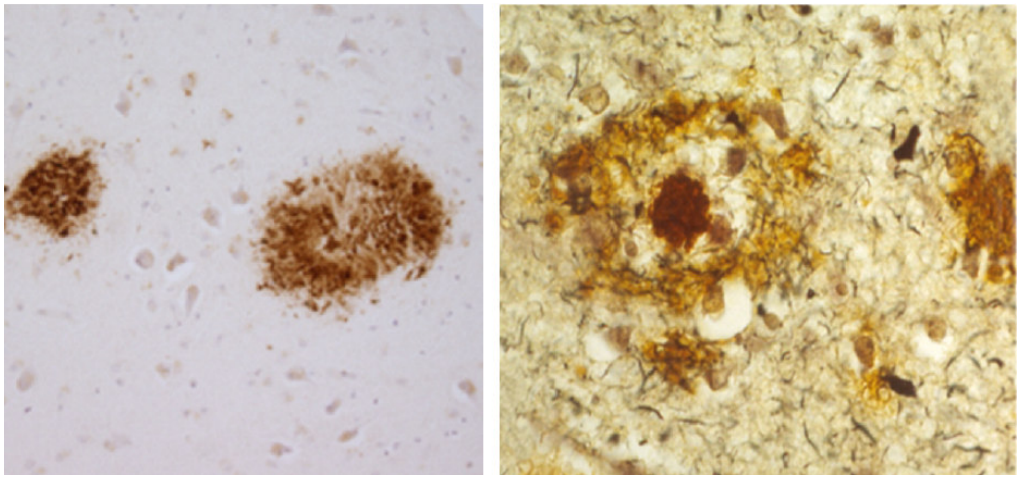

Figure 2: Amyloid deposits. Diffuse (**A**) and classical (**B**) plaques are the most common forms of Aβ-deposits in AD. They are clearly distinguished morphologically. **A**: Diffuse plaques consist of non-compact Aβ-deposits and represent the first type of plaques seen in the human brain. **B**: Classical plaques are characterized by a compact amyloid cored and a surrounding halo of diffuse Aβ representing the "mature" form of senile plaques.

Diffuse plaques are characterized by non-compact deposits (Fig. 2A). The size varies from a few microns to more than a hundred microns in diameter and they exhibit irregular contours. In the absence of neuritic changes different types of diffuse plaques can be distinguished by the presence of full length or N-terminal truncated Aβ-peptides and ApoE. Neuritic changes in diffuse neuritic plaques are classified according to the proteins seen in the dystrophic neurites: APP, PHF and α-synuclein (Wang and Munoz, 1995; Thal et al., 2006a). Diffuse plaques are frequently seen in elderly non-demented individuals. Thereby, non-neuritic diffuse plaques are the first type of plaques seen in the brain during the evolution of AD-related Aβ-deposition. They are discussed to represent the earliest stage of plaque formation (Delaere et al., 1990).

Cored plaques, synonymous with classical plaques, are clearly distinguished from diffuse plaques by their morphology (Fig. 2B). Cored plaques are characterized by an amyloid core in the center surrounded by a corona of diffuse Aβ-deposits. Dystrophic neurites positive for APP, PHF, and α-synuclein classify subtypes of cored plaques into APP-type, PHF-type, and α-synuclein-type plaques, respectively. Core-only plaques are represented by a sharply delineated amyloid core without

any surrounded corona. Cored and cored neuritic plaques may represent “mature” forms of plaques that develop from diffuse plaques and occur in late stages whereas diffuse plaques occur in all stages of Aβ-deposition (Masters et al., 1985b; Griffin et al., 1995; Thal et al., 2000b).

Other types of plaques have been also described in the brain: Subpial band-like amyloid, i. e. sharply delineated evenly distributed band-like deposits of Aβ within the subpial portion of the neocortical molecular layer (Braak and Braak, 1991a, 1991b); lake-like amyloid, i. e. sharply delineated, evenly distributed Aβ-deposits (Kalus et al., 1989; Wisniewski et al., 1998); Fleecy amyloid, i. e. cloud-like Aβ deposits diffusely distributed in the internal entorhinal layers (Thal et al., 1999); White matter plaques; and cotton wool plaques, i. e. sharply delineated, evenly distributed Aβ deposits in roundish, cotton wool-like amyloid plaques without amyloid core and without neuritic changes (for review see (Thal et al., 2006a).

1.2.3.1. Cerebral amyloid angiopathy

In addition to senile plaques, deposition of Aβ is also seen in the walls of cerebral blood vessels (Scholz, 1938; Glenner and Wong, 1984). It is known as cerebral amyloid angiopathy (CAA). Although CAA may occur independently of AD, it is seen approximately in 80-100% of all AD cases, particularly in elderly individuals. CAA is a common cause of cerebral hemorrhage in aged individuals (Vinters and Gilbert, 1983). Mutations in the APP gene can lead to CAA with hemorrhage (hereditary CAA with hemorrhage of the Dutch type) (Roos et al., 1991). Aβ deposits are mainly located in small arteries of the leptomeniges and the cerebral cortex. Factors that influence the balance between parenchymal and vascular Aβ-deposition are not fully understood but it seems that ApoE as well as the balance of $A\beta_{1\text{-}40}/A\beta_{1\text{-}42}$ play an important role for cerebrovascular deposition of Aβ (Olichney et al., 2000; Thal et al., 2002c; Herzig et al., 2004). The role of ApoE in vascular Aβ-deposition is supported by the finding of the presumable involvement of ApoE in the perivascular clearance of Aβ (Thal et al.,

2006b). $A\beta_{40}$ represents the major Aβ-protein within vascular Aβ-deposition, in contrast to senile plaques where $A\beta_{42}$ is the major Aβ-form (Gowing et al., 1994).

1.2.3.2. Amyloid deposition in the aging brain and AD

Aβ deposits can be found both in the aging brain and in AD. In non-demented elderly people, AD-related Aβ-deposits are restricted to distinct predilection sites. On the other hand, Aβ-deposits are seen in numerous areas of the brain in AD patients (Arnold et al., 1991; Braak and Braak, 1991b; Bancher et al., 1993; Aging, 1997; Thal et al., 2002a; Thal et al., 2006a). The deposition of Aβ in the non-demented and in the AD brain shows a sequence in which the areas of the brain become step-by-step involved in Aβ-deposition. Five phases of Aβ deposition can be distinguished (Thal et al., 2002a) (Fig. 3). In the first phase diffuse Aβ-plaques are found exclusively in the neocortex in small groups in layers II, III, IV, and V. The second phase is characterized by additional Aβ-deposits in allocortical brain regions, i. e. in the entorhinal region, CA1, and the cingulate cortex. Subcortical areas become involved in phase 3. Aβ-deposits occur in the diencephalic nuclei, the striatum, and the cholinergic nuclei of the basal forebrain. A normal aging brain can show phases 1 to 3. Further brain regions are usually free of Aβ-deposits in non-demented individuals (Thal et al., 2002a).

The involvement of further brain regions is most frequently accompanied with the occurrence of cognitive deficits. In phase 4 several brain stem nuclei exhibit senile plaques as well. The inferior olivary nucleus, the reticular formation of the medulla oblongata, substantia nigra, CA4, the central grey of the midbrain, the colliculi superiors and inferiors, and the red nucleus frequently exhibit Aβ-deposits. Finally, phase 5 is characterized by cerebellar Aβ-deposition. Additionally, the reticular formation of the pons, the pontine nuclei, the central and dorsal raphe nuclei, the locus coeruleus, the parabrachial nuclei and the reticulotegmental nucleus of the pons become involved in β-amyloidosis in this phases as well (Thal et al., 2002a). These phases are the results of a cross-sectional study of

human autopsy brains. Although it is tempting to speculate that they represent the time course of Aβ-deposition, it cannot be excluded that they may show just different pathologies in different individuals.

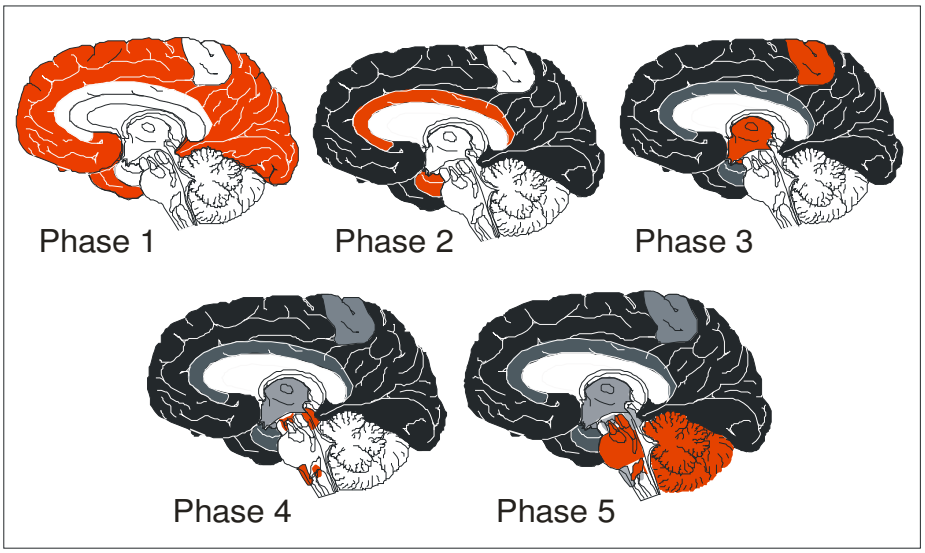

Figure 3: Phases of Aβ-deposition in the human brain. Phase 1 is characterized by neocortical Aβ-deposits. An additional allocortical involvement characterizes phase 2. Phase 3 exhibits additional Aβ-deposits in the diencephalon, and the basal ganglia. Phase 1-3 represent the pre-clinical stages of the disease. Clinical stages are characterized by additional involvement of the midbrain and the lower brain stem in phase 4. In phase 5, Aβ deposits also occur in the pons and the cerebellum. Newly involved brain areas are marked in red (from (Thal et al., 2004).

1.3. Neurofibrillary pathology

Neurofibrillary pathology (NFP) is the second major histopathological hallmark of AD and includes NFT, neuropil threads and dystrophic neurites in neuritic plaques (Fig. 4).

NFT are argyrophilic fibrils in the perikarya and proximal dendrites of neurons (Alzheimer 1907). The major structural component is the tau protein (Grundke-Iqbal et al., 1986; Kosik et al., 1986), a protein that binds to microtubules in the non-phosphorylated state and regulates the axonal transport (Mandelkow and Mandelkow, 1998). However, abnormal phosphorylation of tau results in a

disassembly of normal microtubules, leading to the formation of paired helical filaments and finally, NFTs (Mandelkow and Mandelkow, 1998).

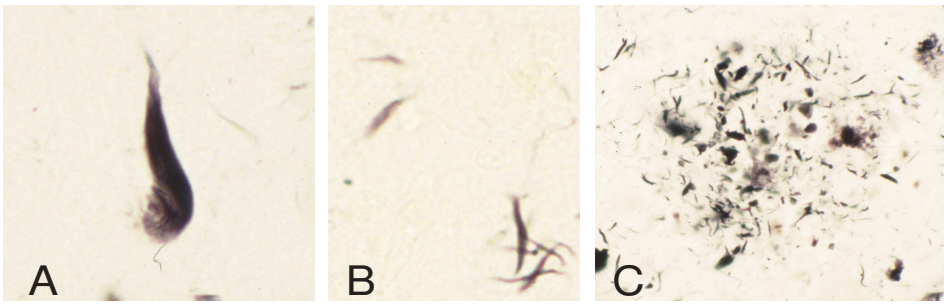

Figure 4: Neurofibrillary pathology: Neurofibrillary tangles (**A**), neuropil threads (**B**) and dystrophic neurites (**C**) of neuritic plaques represent the neurofibrillar pathology in AD.

Neuropil threads are fibrillary aggregates of abnormal phosphorylated tau within dendrites (Braak and Braak, 1991b).

The term neuritic plaque summarizes diffuse and cored plaques which exhibit dystrophic neurites (Braak and Braak, 1991b; Thal et al., 2006a).

1.3.1. Staging of neurofibrillary pathology

Similar to Aβ deposits, NFP also occurs frequently in normal aging. In these individuals NFP is restricted to entorhinal and limbic areas in non-demented elderly. The development of NFP in the brain follows a characteristic sequence in which the different areas of the brain become hierarchically involved. This sequence is divided in six stages, i.e. the Braak-stages (Fig. 5) (Braak and Braak, 1991b). The stages I and II are characterized by a mild to severe alteration of the transentorhinal region and the entorhinal cortex (Entorhinal stages I-II). Stages III-IV represent the limbic stages. In addition to the transentorhinal and entorhinal region, there is an involvement of the Ammon's horn and an expansion into the gyrus parahippocampalis. Finally, stage V-VI, show further expansion in the

isocortical parts of the brain (Braak and Braak, 1991b). Stages IV-VI are frequently associated with cognitive decline (Thal et al., 2002a). Similar to the phases of Aβ-deposition, the Braak-stages are the result of cross-sectional studies, and it is not clear whether the hierarchical degeneration of neurons represents the time course of the disease progression or just different pathologies in different individuals. However, the Braak stages correlate with the phases of Aβ-deposition (Thal et al., 2002a).

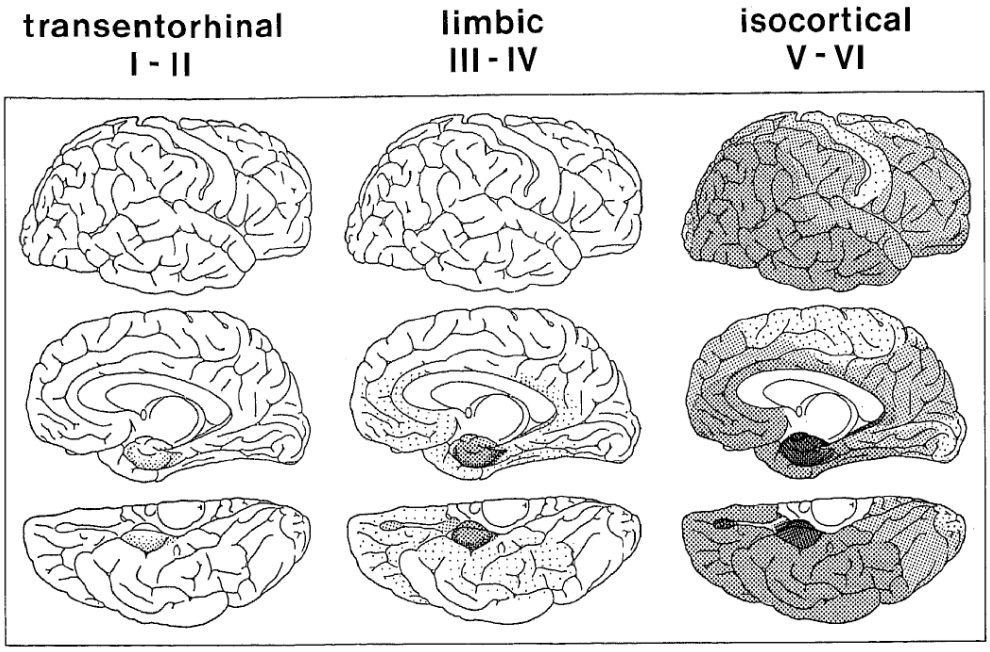

Figure 5: Distribution of the neurofibrillary pathology in human brain is divided in six stages. Stage I-II showed NFP within the transentorhinal and entorhinal regions. Severe involvement of the entorhinal and transentorhinal pre-α layers as well as NFP in the hippocampus and other limbic areas characterize stages III-IV. Finally, additional isocortical NFP characterizes stage V-VI (from (Braak and Braak, 1991b).

1.4. Neuronal loss and synaptic loss in AD

Neuronal loss is well documented in AD (Duyckaerts and Dickson, 2003). In the hippocampus the density of neurons decreases up to 57% and is highly correlated with the expansion of NFT pathology (Ball, 1977). Since AD is a slowly progressive neurodegenerative disorder, only a few cells

undergo apoptosis at a given point in time as seen in a cross sectional autopsy study by quantification of caspase 3 positive neurons (Stadelmann et al., 1999). Multiple studies indicate that caspases are involved in AD related neuronal death (Mattson, 2000; Chan et al., 2002; Haughey et al., 2002). Vulnerable neuronal populations differ in normal aging and AD (Braak and Braak, 1991b; Morrison and Hof, 1997). While the hilus of the dentate gyrus and subiculum show neuronal loss in normal aging, the CA1 region exhibits severe neuronal loss mainly in AD patients (West, 1993; West et al., 1994). In the entorhinal cortex neuronal loss may reach 90% in advanced AD cases. In the isocortex a large number of neurons degenerate (Terry et al., 1981; Terry et al., 1987). Pyramidal cells in layers III, mainly involved in corticocortical connections, and in layers V are most vulnerable in AD patients (Alzheimer, 1907; Terry et al., 1981; Braak and Braak, 1991b; Duyckaerts and Dickson, 2003). In Down-syndrome patients, i. e. trisomy of the chromosome 21 resulting in the overexpression of APP, the number of neurons in layer III and V in the frontal neocortex is reduced as well (Davidoff, 1928). Moreover, a region-specific reduction of corpus callosum is seen in AD patients indicating the degeneration of commissural fibers (Hampel et al., 1998). Magnetic resonance imaging based corpus callosum measurements, thus, may reflect the specific loss of large pyramidal neurons in the cortical layers III and V of the frontal and parieto-occipital association areas (Hampel et al., 1998). In so doing, there is a selective vulnerability of distinct types of neurons in AD. Synaptic and dendritic loss has been described in the hippocampus and in neocortex of AD patients (de Ruiter and Uylings, 1987; Catala et al., 1988; Scheff et al., 1990). The decrease of cortical synaptic density is reflected by changes in the presynaptic marker synaptophysin and correlates with cognitive decline in AD patients (DeKosky et al., 1996).

1.5. Transgenic mouse models for Alzheimer's disease

Mice expressing pathogenic mutations of human genes have become a very powerful tool for biomedical research and drug discovery. The identification of familiar AD-linked mutation in APP, led to the generation of different mouse models overexpressing human mutant and non-mutant APP. Today, there are more than 40 different types of APP-transgenic mice available and more than 100 transgenic mice expressing mutation in other genes related with AD (APOE, BACE, PS1, PS2, and tau). The development of transgenic mice carrying different mutations and/or the use of different promoters results in mice with various phenotypes. These different types of mice allow the analysis of different aspects of Aβ and AD-related pathology. A summary presenting the most important mouse models is provided in table 2.

The first APP transgenic mouse model showing significant amyloid pathology was published in 1995 (Games et al., 1995). The expression of human APP (hAPP) with the Indiana-mutation is driven by the platelet derived growth factor-β (PDGF-β) promoter (PDAPP mouse). Mutant APP expression in PDAPP mice is approximately 10-fold higher than the endogenous APP levels. First plaques are observed at 6 to 9 months of age in the hippocampus and cerebral cortex, and both the number and the density of plaques increase with the age. Phosphorylated neurofilament immunoreactive dystrophic neurites are detected in the rim of plaques at 10 to 12 months of age, while phosphorylated tau-immunoreactive dystrophic neurites are observed after 14 months of age (Masliah et al., 2001). The dystrophic plaque neurites do not contain filamentous tau, NFT is not observed. Although there is a significant amyloid deposition, with decreased synaptic and dendritic densities in PDAPP mice, no neuronal loss has been described in these mice (Irizarry et al., 1997; Wu et al., 2004). PDAPP mice have both age-independent and age-dependent memory deficits. Deficits in the spatial discrimination tests are age-independent and began prior to amyloid deposition (Dodart et al., 1999). On the other hand, amyloid load correlates with an age-dependent decrease in spontaneous object-recognition

performance (Dodart et al., 1999) and deficits in spatial learning in the Morris water maze from 13 months of age (Chen et al., 2000).

Table 2. Summary of the most relevant APP transgenic mice.

Transgenic line	Transgene/ Promoter	Behavioural phenotypes	Neurological characteristic	Deficits	References
PDAPP	Minigene encoding codon 717 V to F mutation/modified hAPP introns 6, 7, 8 in construct resulted in expression of 770, 751 and 695 isoforms of human APP/PDGF-β promoter.	Significant impairment on a variety of different learning and memory tests. Age-independent and age dependent memory deficits.	Aβ deposits, neuritic plaques, synaptic loss, astrocytosis and microgliosis.	No NFT or neuronal loss	(Games et al., 1995)
APPSWE (2576)	Human AP695 cDNA with KM670/671NL/ hamster prion protein gene promoter	Memory deficits seen in 9-10 month old tg mice.	Aβ deposits at 9-12 months. Gliosis, dystrophic neurites containing phosphorylated tau. Localized neurons and synapse loss.	No NFTs. Aβ peptide may be modified/processed differently to those in AD	(Hsiao et al., 1996)
APP23	APP_{751}Swedish/ murine Thy-1.2 promoter	Learning impairment in Morris water maze and a passive avoidance paradigm	7x over expression of APP mRNA. Aβ deposits at 6 months, by 24 months in neocortex and hippocampus. Inflammation, neuritic and synaptic degeneration and tau hyperphosphorylation. Evidence for CAA.	No NFTs.	(Sturchler-Pierrat et al., 1997)
APPLondon V717I	Human APP695 cDNA with V717I/ mouse Thy-1 gene. The thymus specific regulatory elements in intron 3 are thereby deleted, making the resulting promoter "neuron-specific".	Decreased exploration, increased neophobicity, increased male aggressivity.	Amyloid plaques and cerebrovascular angiopathy - onset 10-12 months, cholinergic fiber distortion.	No NFTs.	(Moechars et al., 1999)
PDAPPSwInd (J20)	Tg construct: hAPPSwInd Promoter: PDGFB Injected: C57BL/6 x DBA/2F2 embryos	WM spatial memory retention, acquisition, deficits 6-7 months (Palop et al., 2003).	Total Aβ and Aβ42 overexpression in neocortical and hippocampus. High levels of $Aβ_{42}$ resulted in age-dependent formation of Aβ plaques in mutant hAPP mice but not wild-type hAPP mice	No NFTs.	(Mucke et al., 2000)
TgCRND8	APPSwe/Ind (KM670/671NL+V717F)/ hamster prion promoter	At 3 months impairment in acquisition and learning reversal in memory version of the Morris water maze. Immunization against Aβ42 offset learning impairment.	Aβ deposits at 3 months of age, by 10 weeks levels of $Aβ_{40}$ and $Aβ_{42}$ peptides 5-fold higher than endogenous mouse-APP. Dense-cored plaques and neuritic pathology evident from 5 months of age. Activated microglia appears concurrently with plaques.	No NFTs. Rapid progression does not mirror typical AD time course.	(Chishti et al., 2001)
APP/PS-1	hAPP (KM670/671NL and V717I, Thy-1 promoter) hPS-1 (M146L, HMG promoter).	Not reported.	High levels of $Aβ_{40}$ and $Aβ_{42}$ before plaque deposition. Hippocampal pyramidal cell loss. Astrocytosis in the surrounding of the plaques.	No NFTs.	(Wirths et al., 2001)
APPsw/Tau (P301)/PS1 (M146V) 3x tg	$APP_{Sw(KM670/671NL)}$ $Tau_{(P301L)}$/Thy-1.2 promoter/ co-microinjected into pronuclei of embryos of $PS1_{M14V}$KI mice	Cognitive impairments by 4 months as retention/retrieval deficits occur prior to any plaques or tangle pathology. Early cognitive deficits can be reversed by immunotherapy.	Age related and progressive plaques and tangles. Deficits in LTP correlate with accumulation of intraneuronal Aβ. Tau and APP expression doubled in homozygous mice in hippocampus and cerebral cortex. Hippocampal neuronal loss.		(Oddo et al., 2003b)

One year later, Hsiao et al. (Hsiao et al., 1996) generated the Tg2576 mouse. This mouse expresses the most abundant APP isoform, APP695 with the Swedish double mutation K670N/M671L, under the control of the hamster prion protein promoter (hPrP). These mice overexpress mutant APP 5-fold over the endogenous mouse APP expression. First amyloid plaques are detected at 9 to 12 months in the frontal, temporal, entorhinal cortex, hippocampus, presubiculum, subiculum in a similar distribution as in PDAPP mice. Phosphorylated tau is detected in dystrophic neurites, but no tau filaments and no NFTs (Tomidokoro et al., 2001a; Tomidokoro et al., 2001b). Although these mice do not show significant neuronal loss, Spires et al. (Spires et al., 2005) showed pronounced synaptic loss near senile plaques. This disruption appeared to extend beyond plaques. 9-10 months old Tg2576 mice develop memory deficits (Hsiao et al., 1996). These behavioural alterations correlate with the development of amyloid plaques and with impaired long-term potentiation (Hsiao et al., 1996).

Another APP transgenic mouse model, the APP23 mouse, was developed by Sturchler-Pierrat and colleagues in 1997. In contrast to Tg2576 and PDAPP mice, APP23 mice express the 751 amino acid isoform of hAPP (hAPP751) with the Swedish mutation (K670N, M671L)(sweAPP) driven by a neurons specific Thy 1 promoter. Transgene derived APP levels exceed the endogenous APP by 7-fold (Andra et al., 1996; Sturchler-Pierrat et al., 1997). Histopathologically, these mice are characterized by progressive Aβ-deposition. The first deposits appear at 5-6 months of age (Sturchler-Pierrat et al., 1997; Thal et al., 2006a). In addition to parenchymal Aβ accumulation, CAA leads to vessel wall degeneration, often associated with hemorrhage (Winkler et al., 2001). Less frequently CAA-associated vasculitis and minor aneurysms were seen (Winkler et al., 2001). Activated microglia and astrocytes are associated with Aβ-plaques in these mice (Sturchler-Pierrat et al., 1997). Dystrophic neurites and tau protein hyperphosphorylation has also been described (Sturchler-Pierrat et al., 1997), although NFT are not found. APP23 mice show a selective neuronal death in the hippocampus section CA1 (Calhoun et al., 1998), which is not observed in Tg2576 and PDAPP mice. APP23 mice show an

age-dependent decline of spatial memory capacities. From 3 months of age, these mice displayed major learning and memory deficits. In addition to the cognitive deficits, APP23 mice also show disturbed activity patterns. At 6 months of age lower activity levels and different exploration behaviour are seen compared to control mice (Kelly et al., 2003; Van Dam et al., 2003).

Since APP transgenic mice do not show the full spectrum of AD-like pathology, double and triple transgenic mice have been developed with the aim of obtaining a mouse model showing the full spectrum of AD pathology. Double transgenic mice expressing a double mutation in APP (Swedish APP mutation $APP_{K670N, M671L}$ and APP_{V717I} under the mouse Thy-1 promoter) and mutant presenilin-1 (PS-1 M146L under the pHMG promoter) showed for example a significant age-related loss of hippocampal pyramidal cells. NFTs were not seen in these mice. Since the PS-1 mutation itself may accelerate age-related degeneration, it is difficult to clarify the role of Aβ for neurodegeneration in this APP/PS-1 mouse model.

In 2003, Oddo et al (2003b) reported a transgenic mouse model for AD that develops both plaques and NFT pathology in AD-related brain regions, a triple transgenic mouse (3xTg-AD) harbouring $PS1_{M146V}$, APP_{Swe}, and tau_{P301L} trangenes (Table 2). Diffuse and fibrillar Aβ-aggregates are seen in this mouse model (Oddo et al., 2003b). Aβ-aggregates are initially seen in neocortical areas and also develop Aβ-deposits in limbic areas with the age. In contrast, tau aggregates occur first in the hippocampus and then expand into further cortical regions (Oddo et al., 2003a). Both Aβ-deposition and tau-aggregates follow a very similar expansion pattern as described in AD patient. In 3xTg-AD mice intracellular Aβ is the first manifestation of pathology and extracellular Aβ-deposits occur prior to the aggregates of abnormal tau protein (Oddo et al., 2003a). Synaptic dysfunction, including LTP deficits, occurs in an age related manner but prior to the onset of Aβ-pathology. Moreover, the occurrence of intraneuronal Aβ-immunoreactivity in CA1 pyramidal neurons correlates with impairments in synaptic plasticity including deficits in LTP. Therefore, 3xTg-AD mice reproduce the

neuropathology of AD best and became a very useful model for analyzing the relation between the different proteins involved in AD. However, the upregulation of three mutant proteins at a time does not allow the investigation of the pathological effects of one of these proteins alone.

In so doing, the APP23 mouse is the only transgenic mouse model for AD that overexpresses a distinct protein, sweAPP, and exhibits selective neuronal death in a brain region that is affected in AD. Thus, this mouse model allows the investigation of Aβ-induced neurodegeneration in the absence of other contributing factors such as the expression of mutant PS1 or mutant Tau protein.

2. AIMS OF THE STUDY

In order to clarify the neurodegenerative mechanisms involved in AD it is essential to identify the proteins or protein aggregates that induce nerve cell degeneration. The amyloid hypothesis indicates that Aβ has an essential pathogenetic role in AD (Hardy et al., 1989; Hardy, 1990). Therefore, it needs to be clarified whether Aβ is capable of altering different types of neurons in a model similarly as in AD. In the event that Aβ-toxicity is the driving force for AD-related pathology, one would expect Aβ to be capable of inducing degeneration of vulnerable neurons in a mouse model for AD. Although there is increasing evidence that soluble aggregated forms of Aβ are neurotoxic (Kayed et al., 2003; Kokubo et al., 2005b), it is not clear whether these forms of Aβ alter vulnerable neurons selectively and why distinct types of neurons are altered by Aβ whereas others are resistant.

In the human brain Aβ-deposition shows a hierarchical sequence in which the different areas of the brain become step-by-step involved. It is necessary to examine whether this sequence represents the time course of AD-related Aβ-deposition or just different pathologies in different individuals.

To address these questions this study was aimed at,

1) examining that the step-by-step development of Aβ-deposition in the brain represents the time course of cerebral β-amyloidosis or just different pathologies in different individuals,
2) clarifying which Aβ forms are capable of inducing neurodegeneration,
3) identifying whether Aβ is capable of inducing selective degeneration of distinct types of neurons,
4) correlating the effects of Aβ-induced neurodegeneration with the Aβ content, the Aβ plaque load, and the overall distribution of Aβ plaques in the mouse brain, and
5) comparing Aβ induced neurodegeneration in the mouse model with that in AD brain.

3. MATERIAL AND METHODS

3.1. Material

3.1.1. Animals

Heterozygous female APP23 and wild-type mice were provided by the Novartis Institutes for Biomedical Research (Basel, Switzerland) free of charge.

Age (months)	3	5	11	15	26
Wild-type	n = 8	n = 13	n = 14	n = 9	n = 20
APP23	n = 12	n = 16	n = 13	n = 15	n = 16

3.1.2. Consumables

All consumables used for this study were purchased from the following companies: LaboMedic (Bonn, Germany), VWR International (Darmstadt, Germany), and Schleicher & Schuell GmbH (Dassel, Germany).

3.1.3. Chemicals

All the chemicals used for this study were purchased from the following companies: Invitrogene (Karlsruhe, Germany), Merck (Darmstadt, Germany), Molekularbiologisches & biochemisches Labor (Bielefeld, Germany), Molecular Probes (Eugene, OR, USA), peqLab (Erlangen, Germany), Roche (Mannheim, Germany), Sigma (Taufkirchen, Germany).

3.1.4. Solutions

For genotyping:

- DNA digestion buffer

Components	Concentration	Company
Tris HCl	50mM	Sigma, Taufkirchen, Germany
EDTA	100 mM	Sigma, Taufkirchen, Germany
SDS	0,5 %	Sigma, Taufkirchen, Germany

- PCR reaction mixture

Components	Concentration	Company
dNTPs-mix	0.2mM	peqLab, Erlangen, Germany
$MgCl_2$	1mM	Invitrogene, Karlsruhe, Germany
Forward primer	5pmol/µl	Invitrogene, Karlsruhe, Germany
Reverse primer	5pmol/µl	Invitrogene, Karlsruhe, Germany
Taq polymerase	1.25U/50µl	Invitrogene, Karlsruhe, Germany
ddH_2O	according to final concentration	Delta Select GmbH, Pfullingen, Germany

- 50x TAE (Tris Acetate EDTA), pH 8.5

Chemicals	Amount	Company
TRIS Base	2M	Sigma, Taufkirchen, Germany
Glacial acetic acid	57%	Sigma, Taufkirchen, Germany
$Na_2EDTA\ 2H_2O$	0.1M	Sigma, Taufkirchen, Germany
ddH_2O	To 1 liter	Millipore GmbH, Schwalbach, Germany

- 2% agarose gel

Components	Amount	Company
Agarose	2 %	peqLab, Erlangen, Germany
EtBr	0.6M	Sigma, Taufkirchen, Germany
TAE 1x	100 ml	See 50x TAE

For the DiI tracing method:

- 0.05M Tris Buffer Solution (TBS), pH 7.5

Components	Amount	Company
Trizma Base	0.05M	Sigma, Taufkirchen, Germany
NaCl	0.15M	Sigma, Taufkirchen, Germany
HCl	4.4%	Sigma, Taufkirchen, Germany
ddH_2O	To 1 liter	Millipore GmbH, Schwalbach, Germany

- 0,2M Phosphate buffer solution (PBS), pH 7.6

Components	Amount	Company
Na_2HPO_4	0.16M	Sigma, Taufkirchen, Germany
NaH_2PO_4	0.02M	Sigma, Taufkirchen, Germany
ddH_2O	To 1 liter	Millipore GmbH, Schwalbach, Germany

- 2.6 % Phosphate buffer paraformaldehyde solution (PFA), pH 7.6

Components	Amount	Company
PFA	2.6 %	Sigma, Taufkirchen, Germany
PBS 0.2M, pH 7.6	500ml	See PBS solution
ddH_2O	500ml	Millipore GmbH, Schwalbach, Germany

26g PFA in 500 ml dH_2O solution, heat to 60ºC, neutralized with NaOH 1M, add 500ml of PBS 0.2M, adjust pH to 7.6.

- Perfusion solution

Components	Amount	Company
heparin	0.5%	Roche, Mannheim, Germany
in TBS 0.05M pH 7.4	To 1 liter	See TBS solution

- Tracing solution

Components	Concentration	Company
Iodocetic acid	0.8%	Sigma, Taufkirchen, Germany
Sodium periodate	0.8%	Sigma, Taufkirchen, Germany
DL-Lysine	0.1M	Sigma, Taufkirchen, Germany
in PFA solution	To 1 liter	See PFA solution

For immunohistochemistry:

- Reduction solution

Components	Concentration	Company
Methanol	10%	Merck, Darmstadt, Germany
H_2O_2	30%	Sigma, Taufkirchen, Germany
in TBS, pH 7.6	0.05M	See TBS solution

- Blocking solution

Components	Concentration	Company
DL-Lysine	0.1M	Sigma, Taufkirchen, Germany
Triton X	0.25%	Sigma, Taufkirchen, Germany
in BSA	10%	Sigma, Taufkirchen, Germany

3.1.5. Primer sequence of APP and Actin

Gene	Forward primer	Reverse primer	Size (bp)	Company
APP	5'-GAATTCCGACATGACTCAGG-3'	5'-GTTCTGCTGCATCTTGGACA-3'	246	Invitrogene, Karlsruhe, Germany
Actin	5'-GACAGGATGCAGAAGGAGAT-3'	5'-TTGCTGATCCACATCTGCTG-3'	146	Invitrogene, Karlsruhe, Germany

3.1.6. Summary table of used antibodies

Antibody	Antigen	Species	Dilution	Pretreatment	Reference	Source
$A\beta_{1-42}$	$A\beta_{1-42}$	Rabbit	1:750	Formic acid	(Wild-Bode et al., 1997)	Gift of C. Haass
MBC40	$A\beta_{32-40}$	Monoclonal	1:20	Formic acid	(Yamaguchi et al., 1998)	Gift of H. Yamaguchi
MBC42	$A\beta_{37-42}$	Monoclonal	1:200	Formic acid	(Yamaguchi et al., 1998)	Gift of H. Yamaguchi
22C11	N-Terminal of APP	Monoclonal	1:75	no	(Weidemann et al., 1989)	Chemicon
GAP 43	GAP43	Rabbit	1:75	no	(Masliah et al., 1992a)	Chemicon

3.1.7. Equipment

Centrifuge	Eppendorf 5417R (Eppendorf, Hamburg, Germany)
Injectomat	Injectomat 2000 (Fresenius Homo Care, Alzerau-Hörstein, Germany)
Magnetic stirrer	Magnetic stirrer (Heidolph Instruments, Solingen, Germany)
Microscopes	Fluorescence Microscope Leica DMLB (Leica, Bersheim, Germany) Scanning Confocal Microscope Leica TSC NT (Leica, Bersheim, Germany) Zeiss Stemi 200C Microscope (Carl Zeiss Lichtmikroskopie, Göttingen, Germany)
Oven	T6, Kendro Laboratory products (Langenselbold, Germany)
pH-meter	pH-meter 210 (Hanna Intruments, Kehl am Rhein, Germany)

Scale	Scale (Kern & Sohn GmbH, Balingen-Frommern, Germany)
Softwares	Axiovision AC 4.2 image analysis software (Carl Zeiss Lichtmikroskopie, Göttingen, Germany) CorelDRAW Graphics Suite 12 (CorelDRAW, Unterschleissheim, Germany EndNote v8 (Thomson ISI ResearchSoft, Philadelphia, PA, USA) Image Expert™ Software (Bio-Rad Laboratories GmbH, Munich, Germany) Image J, Imaging Processing and Analysis Software (NIH, Bethesda, MD, USA) Leica FireCam Software(Leica, Bersheim, Germany) Leica TCS Software (Leica, Bersheim, Germany) LogXact 5.0 Software (Cytel Software Corporation, Cambridge, MA, USA) Microsoft Office 2003, Microsoft Deutschland GmbH, Unterschleissheim, Germany) SPSS software (Chicago, IL, USA)
Thermocycler	Thermocycler T1 (Biometra, Goettingen, Germany)
Thermomixer	Thermomixer Comfort (Eppendorf, Hamburg, Germany)
Transilluminator	BioRad Gel Doc1000 (Bio-Rad Laboratories GmbH, Munich, Germany)
Vibrotome	Leica VT1000S (Leica, Bersheim, Germany)
Vortex	Vortex-Genie 2 (Scientific Industries, Inc., NY, USA)

3.2. Animal models

APP23 mice were generated by The Novartis Institutes for Biomedical Research (Basel, Switzerland) as previously described (Sturchler-Pierrat et al., 1997) and continuously back-crossed to C57BL/6. An expression construct containing a murine Thy-1 promoter was used to drive neuron-specific expression of human mutant APP751 with the Swedish double mutation 670/671 KM -> NL. Heterozygous female APP23 mice and female wild-type littermates were analyzed (see 3.1). All mice

were kindly provided by Novartis Institutes for Biomedical Research (Basel, Switzerland). Genotype information was provided.

3.3. Confirmation of APP23 mice genotype

To confirm the genotype of each mouse polymerase chain reaction (PCR) analysis of frozen tail samples was performed. Tail samples were taken immediately before starting perfusion fixation. A sample from each mouse was digested with 0.5% Proteinase K (Invitrogen, Karlsruhe, Germany) in DNA digestion buffer (see materials), overnight at 55ºC in a thermocycler (Biometra, Goettingen, Germany). On the next day samples were centrifuged (13000 rpm/ 10 min./ 4ºC) (Eppendorf, Hamburg, Germany). The supernatants were transferred to tubes containing 500µl of isopropanol (Merck, Darmstadt, Germany) and centrifuged (13000 rpm/ 10 min./ 4ºC). After removal of the supernatant 500µl of 70% ethanol (Merck, Darmstadt, Germany) was added, samples were vortexed and centrifuged (13000 rpm/ 10 min./ 4ºC). Supernatant was discarded. After the pellet was dried it was resuspended in 140 µl of Millipore water.

PCR reaction mixture was prepared as indicated above (see materials) including APP primers. 5µl of DNA per mouse was mixed with 20 µl of PCR reaction mixture. PCR was run with the optimized conditions mentioned below. Amplification of Actin gene was carried out as internal positive control.

The optimized conditions for human APP gene PCR were: preheating at 94ºC, followed by 94°C for 45 sec., 58°C for 45 sec., 72°C for 45 sec., during 35 cycles, followed by 72°C for 5 min., and stored at 4°C.

The PCR reaction products were analyzed on ethidium bromide (EtBr) stained 2% agarose (peqLab, Erlangen, Germany) gels. The DNA samples were loaded into wells of the gel. pUC 19 MsP I was used as DNA-marker (Molekularbiologisches & biochemisches Labor, Bielefeld, Germany).

Electrophoresis was run with 1xTAE running buffer under voltage to 180V until the dye marker was migrated appropriately. After separation of the PCR products the EtBr-stained gels were transferred to the ultraviolet (UV) transilluminator (Bio-Rad Laboratories GmbH, Munich, Germany) to demonstrate visible reaction products and were photographed using digital camera system and Image Expert™ Software (Bio-Rad Laboratories GmbH, Munich, Germany).

3.4. Western blot analysis

For the confirmation of APP overexpression in APP23 mice western blot data were kindly provided by The Novartis Institutes for Biomedical Research (Basel, Switzerland).

Forebrain hemispheres (excluding olfactory bulb, cerebellum and brainstem) were weighed and homogenized by sonication in 10 volumes of buffer (20 mM Tris-HCl pH 7.6, 137 mM sodium chloride, protease inhibitor cocktail (Complete, Roche Molecular Biochemicals, Mannheim, Germany)). For immunoprecipitation, homogenates were supplemented with 1% sodium dodecyl sulfate, heated to 95°C for 3 minutes, diluted with 9 volumes of homogenization buffer and cleared by centrifugation at 15°C for 15 minutes at 20000xg. Aβ-peptides were immunoprecipitated using the monoclonal antibody β1 reacting with the amino-terminus of Aβ (Schrader-Fischer and Paganetti, 1996) and protein G coated magnetic beads (Dynal Biotech, Hamburg, Germany). Precipitates or whole homogenates were separated on 10% Tris-bicine gels with 8 M urea as described (Klafki et al., 1996; Staufenbiel and Paganetti, 1999). In this system, $A\beta_{1-40}$ migrates slower than $A\beta_{1-42}$. Proteins were transferred to Immobilon-P membranes (Millipore, Carrigtwohill, Ireland). Aβ-peptides were fixed to the membrane by heating it to 95°C for 3 minutes in phosphate buffered saline (PBS) (Sigma, Taufkirchen, Germany) (Staufenbiel and Paganetti, 1999). Full length APP was detected with rabbit antiserum APP-C8 raised against the carboxy-terminal amino acids of APP (Schrader-Fischer and

Paganetti, 1996) which are identical in mice and humans. Transgene derived APP and Aβ were detected with the monoclonal antibody 6E10 (Signet, MA, USA). After incubation of the blots with the appropriate peroxidase coupled secondary antibodies (Jackson Immunoresearch, Soham, UK and Sigma, Taufkirchen, Germany), proteins were detected by visualizing chemiluminescence (ECL advance, Amersham Pharmacia Biotech, NJ, USA) on autoradiographic films (Hyperfilm ECL, Amersham Pharmacia Biotech, NJ, USA).

3.5. Enzyme linked immunoabsorvent assay (ELISA)

Quantification data of the Aβ levels were kindly provided by The Novartis Institutes for Biomedical Research (Basel, Switzerland). Statistical analysis was performed in the Department of Neuropathology, University Hospital of the Rheinische Friedrich-Wilhelms-University of Bonn, Bonn (Germany).

For quantification of Aβ levels by ELISA, forebrain homogenates from APP23 mice of each age group (3 months: n=6; 5 months: n=6; 11months: n=4; 15 months: n=7) were supplemented with concentrated formic acid to a final concentration of 70%. After 15 minutes of incubation on ice and mixing every 5 minutes, the samples were neutralized by addition of 19 volumes 1 M Tris base supplemented with protease inhibitor cocktail. The extracts were cleared by centrifugation (20000xg for 15 min at 4°C). Supernatants from young (3 or 5 months) APP23 mice were directly loaded on sandwich ELISA plates for quantification of Aβ peptides ($A\beta_{1-40}$: ELISA from IBL, Hamburg, Germany; $A\beta_{1-42}$: ELISA from Innogenetics, Ghent, Belgium). Supernatants from 11 and 15 months old APP23 mice were diluted as necessary in dilution buffers supplied with the ELISAs. Standard curves were prepared with synthetic peptides $A\beta_{1-40}$ and $A\beta_{1-42}$ purchased from Bachem (Bubendorf, Switzerland) and diluted in extracts of non-transgenic mouse forebrain prepared in parallel as described above. Each sample was analyzed in duplicate.

3.6. Labeling of commissural neurons

To detect Aβ-induced neuronal alterations in APP23 mice we examined commissural neurons of the frontocentral cortex known to be vulnerable in AD (Alzheimer, 1907; Terry et al., 1981; Braak and Braak, 1991b; Duyckaerts and Dickson, 2003). The DiI-tracing method was used to study the morphological integrity of the commissural neurons. To confirm that the staining pattern seen with the DiI-tracer is not the result of methodological limitations of the DiI-method, a second tracing method in vivo tracing with biotinylated dextrane amine, was used.

3.6.1. DiI tracing

Commissural neurons of the frontocentral cortex were labeled using DiI (1,1'-dioctadecyl-3,3,3',3'-tetramethylindolcarbocyanine perchlorate) as a tracer. DiI is a highly fluorescent lipophilic carbocyanine that becomes incorporated into the cell membrane of those cells that are in contact with the dye (Haugland, 2005). Other cells are not labeled. It is used for anterograde and retrograde tracing of neuronal cells in vivo (Honig and Hume, 1986, 1989; Wouterlood, 1993) and in fixed tissues (Godement et al., 1987; Baker and Reese, 1993; Wouterlood, 1993). Once applied, the dye diffuses laterally within the plasma membrane of the cells in contact with the dye, resulting in a staining of the entire cell (Haugland, 2005). This dye allows precise Golgi-like tracing of neurons in postmortem fixed tissue in a quality similar to in vivo tracing methods using rhodamine tracers even in only weakly traced neurons (Galuske and Singer, 1996).

For DiI-tracing brains of 3, 5, 11, and 15 months old APP23 (3 months: n=6; 5 months: n=9; 11 months: n=8; 15 months: n=8) and wild-type mice (3 months: n=6; 5 months: n=12; 11 months: n=13; 15 months: n=9) were studied. Animals were treated in agreement with the German law on the use of laboratory animals. Mice were anesthetized. Perfusion was performed transcardially with Tris buffered

saline (TBS) supplemented with heparin (pH 7.4) followed by the injection of 0.1 M PBS (pH 7.4) containing 2.6% paraformaldehyde (PFA), 0.8% iodoacetic acid, 0.8% sodiumperiodate, and 0.1 M D-L Lysine. The brains were removed in total and postfixed in 2.6% phosphate buffered PFA (pH 7.4) containing 0.8% iodoacetic acid, 0.8% sodiumperiodate, and 0.1 M D-L Lysine (Galuske et al., 2000). Three days later a single crystal (approximately 0.3 mm^3) of the carbocyanine dye DiI (Molecular Probes, Eugene, OR, USA), was implanted into the left frontocentral cortex, 1 mm rostrally from the central sulcus, 2 mm laterally from the middle line and 1 mm deep in the cortex (Fig.6). After incubation in 2.6% phosphate buffered PFA for at least 3 months at 37°C, 100 µm thick coronal vibratome sections were cut. Sections were mounted in TBS for microscopic analysis.

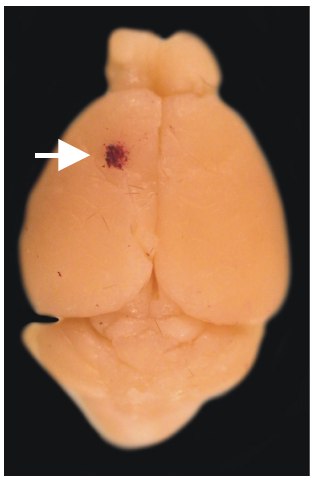

Figure 6: Application site of the DiI tracer in the mouse brain. The DiI tracer was implanted into the left frontocentral cortex: 1 mm rostrally from the central sulcus, 2 mm laterally from the median sagital plane, and 1 mm deep in the cortex (arrow). In so doing, the tracer was placed into layers I-V of the frontocentral cortex.

3.6.2. In vivo tracing with biotinylated dextrane amine

The technical part of this tracing method was kindly performed by Christine Stadelmann and Angelika Escher at the Department of Neuropathology, Georg-August University, Göttingen (Germany). Microscopic analysis and documentation was performed at the Department of Neuropathology, University Hospital of the Rheinische Friedrich-Wilhelms-University of Bonn, Bonn (Germany).

As a second tracing method to confirm the data with the DiI tracing method, we used a biotinylated dextrane amine (BDA; Molecular Probes; probes.invitrogen.com) tracer for in vivo tracing. BDA is characterized by its high molecular weight, good water solubility, low toxicity, and relative inertness. The α-1,6-polyglucose linkages are resistant to cleavage by most endogenous cellular glycosidases. Thus, BDA is ideally suitable as a long-term tracer for living cells. It stains neuronal processes anterogradely as well as retrogradely (Haugland, 2005).

14-week-old C57Bl/6 mice were anaesthetized with ketamin/rompun and placed in a stereotactic frame. After incision of the skin, a fine hole was drilled into the skull 0.1mm caudal and 0.2mm lateral to bregma. A finely drawn glass capillary was stereotactically placed into the frontal cortex (approximal depth 0.5mm), and 1µl BDA was slowly injected over a 3 minute period. After withdrawal of the capillary, the skin wound was closed by suture, and animals were allowed to survive for 3 days. For tissue sampling, animals were anaesthetized, perfused transcardially with 4% PFA, and dissected. Brain slices were embedded in gloop, a mixture of egg albumin, gelatine, sucrose and gluaraldehyde, and 50µm vibratome sections were cut. BDA was visualized using an avidin-peroxidase based method (vectastain; www.vectorlabs.com) with diaminobenzidine as chromogen. Sections were dehydrated, and coverslipped.

3.7. Microscopic and quantitative analysis of commissural neurons

In layer III of the frontocentral cortex of the right hemisphere, contralateral to the implantation site of the tracer, the morphology of traced commissural neurons was examined. The traced neurons were assigned to different types according to their morphology. Then the number of traced commissural neurons of each type in wild-type mice was compared with that in APP23 mice. For qualitative and quantitative analysis 10 consecutive sections (100 µm thickness each) representing a tissue block of 1 mm thickness were studied for each mouse. Analysis started at the anterior

commissure setting the caudal limit of the investigated tissue block. For each coronal section, the medial boundary of the region investigated was set as the vertical line at the cingulum that separated the cingulate cortex (Cg) from secondary motor cortex (M2) (Fig. 7). The horizontal boundary was set as the horizontal line separating the primary somatosensory cortex (S1) from the insular cortex (I) (Fig. 7).

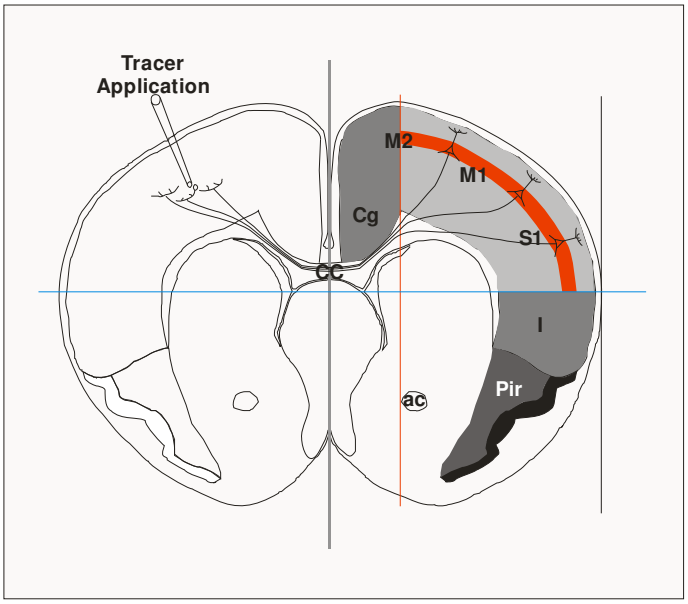

Figure 7: The schematic representation shows a coronal section of the mouse brain at the level of the tracer application site. Layer III commissural neurons within the contralateral frontocentral cortex labeled by the DiI tracer were studied in the secondary and primary motor cortex (M1 and M2) and the somatosensory cortex (S1) (area marked in red) as determined by the following coordinates: the medial boundary was established as the vertical (red) line that separates the cingulate cortex (Cg) from the secondary motor cortex (M2). The horizontal limit was referred to as the horizontal (blue) line that separated the primary somatosensory cortex (S1) from the insular cortex (I).

For the qualitative analysis a laser scanning confocal microscope (Leica TCS NT, Leica, Bensheim, Germany) was used. Stacks of two dimension (2D) images were superimposed digitally using the Image J Imaging Processing and Analysis software (NIH, Bethesda, MD, USA), and three dimension (3D) data sets were generated for the visualization of neurons with their entire dendritic tree.

For quantification of the commissural neurons in APP transgenic and wild-type mice, traced neurons in layer III were counted in the region of interest depicted in Fig. 1 in 10 consecutive sections of the tissue block taken for qualitative and quantitative analysis using a fluorescence microscope (Leica DMLB, Leica, Bensheim, Germany). In so doing, we analyzed a cortex volume of 5-6 mm^3 in each mouse. Mean and median values of the number of traced neurons were calculated and compared between wild-type and APP23 mice. Statistical analysis was performed using the Mann-Whitney U-Test to compare wild-type and APP23 mice. Poisson regression was used to identify differences in the number of traced neurons among the different phases of Aβ-deposition in the brain. Appropriate corrections for multiple testing were made.

3.8. Immunohistochemistry

3.8.1. Aβ-plaques detection and quantification

Immunohistochemistry was performed for the detection and quantification of Aβ-plaques. Free floating sections were incubated with reduction solution (see material) for 30 min. Sections were pretreated for 5 min in formic acid, washed and incubated in blocking solution (see materials) for 90 min. After blocking, sections were incubated with an anti-Aβ antibody (polyclonal rabbit (Wild-Bode et al., 1997), 1/750, 24h at 22°C). The polyclonal antibody detected $A\beta_{1\text{-}40}$ as well as $A\beta_{1\text{-}42}$. To separately detect $A\beta_{40}$ and $A\beta_{42}$ positive material, additional sections were stained with monoclonal antibodies specifically detecting the C-terminus of $A\beta_{40}$ (MBC40 (Yamaguchi et al., 1998), 1/20, 24h at 22°C, formic acid pretreatment) and $A\beta_{42}$ (MBC42 (Yamaguchi et al., 1998), 1/200, 24h at 22°C, formic acid pretreatment). The primary antibody was detected with a biotinylated secondary antibody and the Avidin-Biotin-Peroxidase (ABC) complex (Biomeda, CA, U.S.A), and the reaction was visualized with 3,3-diaminobenzidine (DAB) 3.2mM (Sigma) (Hsu et al., 1981). Sections were washed

in PBS and dH_2O. On glass slides the sections were dried for 30 minutes at 37ºC. Dried sections were put in Xylene for 5 minutes and mounted in Corbit Balsam (Hecht, Hamburg, Germany).

Quantification of the Aβ-plaque load was performed in an area of the frontocentral neocortex in one selected section with plaques using a Zeiss Stemi2000C microscope and Axiovision AC 4.2 image analysis software (Carl Zeiss Lichtmikroskopie, Göttingen, Germany). The Aβ-plaque load was measured for plaques stained with the polyclonal antibody raised against $A\beta_{1-42}$ (Wild-Bode et al., 1997) according to the following determination:

$$\text{Aβ-plaque load} = \frac{\text{area of plaques detected with anti-A}\beta_{1-42}\text{ antibodies in a given region of interest x 100}}{\text{area of the region of interest}}.$$

Mean values of the Aβ-plaque load were compared between 3, 5, 11, and 15 months old APP23 mice with ANOVA.

3.8.2. Staging of Aβ-deposition in APP23 mice

To characterize the expansion of Aβ-deposition in the mouse brain we determined the phases of Aβ-deposition valid for human and APP-transgenic mouse brain (Thal et al., 2002a; Wiederhold et al., 2004; Thal et al., 2006a)(Tab. 3).

Table 3. Phases of Aβ-deposition in APP23 mice brain.

Phase 0	Absence of Aβ deposits
Phase 1	Aβ deposits in the neocortex
Phase 2	Aβ deposits in the neocortex and allocortex
Phase 3	Aβ deposits in the neocortex, allocortex and basal ganglia
Phase 4	Aβ deposits in the neocortex, allocortex, basal ganglia, thalamus and upper brainstem
Phase 5	Aβ deposits in the neocortex, allocortex, basal ganglia, thalamus, upper and lower brainstem and cerebellum

Paraffin embedded tissue from 26 months of age wild type and APP23 mice was additionally included in this study for the characterization of Aβ-deposition in old animals. 4 µm paraffin sections were de-waxed in xylene (5 min, two times), and hydrated through serial alcohols (100%, 2 min., two times; 95%, 2 min.; 90%, 70%, 2 min.; 50%, 2 min.; 30%, 2 min.) to TBS. The same

immunohistochemistry procedure as mentioned above was followed (see 3.8.1). After Aβ-deposits were seen in positive controls, the sections were dehydrated through serial alcohols (30%, 2 min.; 50%, 2 min.; 70%, 2 min.; 90%, 2 min, 95%, 2 min, 100%, 2 min, two times), propanol (2 min), xylene (5 min., two times), and finally mounted with Corbit Balsam (Hecht, Hamburg, Germany).

3.8.3. Analysis of axonal sprouting and axonal damage

Growth association protein 43 (GAP43) is a marker for differentiating neurons and is expressed in elevated levels of developing or regenerating neurites indicating axonal growth (Knyihar-Csillik et al., 1992) as well as of dystrophic neurites in neuritic plaques (Masliah et al., 1992a). APP is also involved in neuritic growth, and it is co-expressed within GAP43 positive in aberrant sprouting neurites (Masliah et al., 1992a). Antibodies against GAP43 and APP were used for studying axonal sprouting. To examine axonal sprouting following axonal or neuronal damage, sections of the area of interest of each mouse were stained with antibodies directed against APP (22C11 (against N-terminal of APP), monoclonal mouse, Chemicon, 1/75, 24h at 22°C) and against GAP43 (polyclonal rabbit, Chemicon, 1/75, 24h at 22°C). Immunohistochemistry was performed as reported in 3.8.1. without formic acid pretreatment.

3.9. Statistical analysis

Statistical analysis was performed using the SPSS 11.0 program (SPSS, Chicago, IL, USA) and LogXact 5.0 software (Cytel Software Corporation, Cambridge, MA, USA). In case of multiple testing p-values were corrected adequately.

4. RESULTS

4.1. Subpopulations of commissural neurons in layer III of the frontocentral cortex

Using retrograde tracing with DiI, three different types of commissural neurons were identified in layer III of the frontocentral cortex in wild-type and APP23 mice at the age of 3-, 5-, 11- and 15-month (Fig. 8A-F). The first type of commissural neurons referred to as type I, showed a DiI-labeled perikaryon of pyramidal shape, an apical dendrite, and multiple basal dendrites with a heavily ramified and spiny dendritic tree. Ramification of the dendrites was characterized by branching of apical and basal dendrites into primary branches exhibiting secondary and tertiary ramifications within layer III (Fig. 8A, D). The basal dendrites were restricted to layers II/III. The apical dendrite showed further ramification within the molecular layer. These type I commissural neurons were predominantly located in the upper part of layer III (Fig. 8D).

The second type of commissural neurons, referred to as type II, exhibited a DiI-labeled perikaryon of pyramidal shape. The apical and basal dendrites were detectable but further ramification and dendritic spines were less frequently observed and the basal dendrites were thicker than those of type I commissural neurons (Fig. 8B, E, F). 3D-reconstruction revealed that the basal dendrites of type II commissural neurons start branching distant from the perikaryon (Fig. 8F). Commissural neurons of type II showed dendritic ramification and spines in the molecular layer as detected by following the apical dendrite in consecutive sections and, thus, represent the classical pyramidal cell morphology. These neurons were most frequently located in the lower part of layer III. Branches of their basal dendrites were also seen in the upper part of layer IV (Fig. 8E, F).

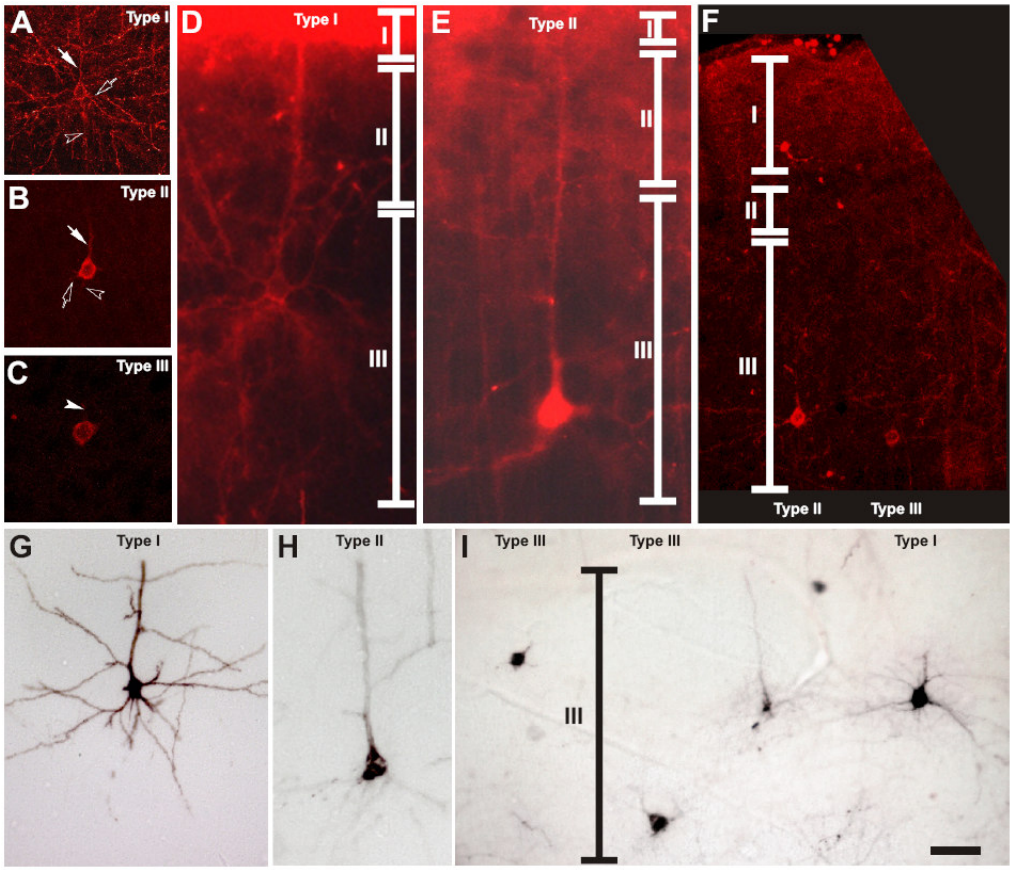

Figure 8: Three types of commissural neurons traced in the frontocentral cortex of wild-type mice. **A**, **B**, and **C** show the typical pattern of these three types of neurons as characterized in 100 µm thick sections after tracing with DiI. Type I commissural neurons are characterized as pyramidal shaped neurons with apical (white arrow) and basal (unfilled arrow) dendrites creating a heavily ramified and spiny dendritic tree showing secondary and tertiary branches within layer III. The axon leaves the perikaryon at the base (unfilled arrow head) (**A**). These neurons are mainly located within the upper part of layer III (**D**). The second type of commissural neurons is the sparsely ramified pyramidal neuron. These neurons are also characterized by a pyramidal cell body and traced apical (white arrow) and basal (unfilled arrow) dendrites. These cells represent the classical pyramidal cells in layer III. There is almost no further ramification of the apical and basal dendrite detectable in this type of neurons within layer III. The basal dendrites start branching distant from the perikaryon as shown in a 3D-reconstruction of serial scans (**F**). The axon is visible at the base of the perikaryon (unfilled arrow head) (**B**). These neurons are preferentially found in the lower part of layer III (**E, F**). **C**: Non-pyramidal commissural neurons referred to as type III commissural neurons, are characterized by a circular cell body. A few dendrites arise from the perikaryon (arrow head). There is no further ramification seen in this type of neurons. The axon is not seen in this section. Type III commissural neurons do not exhibit a distinct predilection site within layer III (**F, I**). **G-I:** Tracing with BDA confirms the staining pattern of the three types of commissural neurons as seen with DiI-tracing. **A-C** show DiI-traced neurons in wild-type mice at 11 months of age, **D-F** in those of 5 months of age. **A-C** and **F** represent 3D-stacks of 16 images of cells in 1,25-1,75 µm distance recorded with the laser scan confocal microscope; **D** and **E** are images digitally captured with the Leica DMLB-microscope. **G-I:** Commissural neurons traced with biotinylated dextrane 3 days before death in wild-type mice of 14 weeks of age mice. Calibration bar in **C** valid for **A**: 55 µm, **B, C**: 40 µm. Calibration bar in **F** valid for **D**, **E**: 35 µm, **F**: 50 µm. Calibration bar in **I** valid for **G-I**: 35 µm.

The third type of commissural neurons, referred to as type III, did not exhibit clearly distinguishable apical and basal dendrites within layer III. Only the cell body with a circular shape was clearly labeled with the tracer. Single, very thin dendrites without spines were labeled in layer III (Fig. 8C, F). These neurons did not show a predilection site in layer III. They occurred in the upper as well as in the lower parts of this cell layer.

In all types of commissural neurons the axon left the neuron at the base and was part of the callosal commissural fiber system. In vivo tracing of wild-type mice with BDA confirmed the staining pattern and the existence of three different types of commissural neurons seen in the DiI-traced sections (Fig. 8G-I).

4.2. Morphological alterations of commissural neurons in APP23 mice

At 3 months of age there were no differences between wild-type and APP23 mice in the morphology of the commissural neurons (Fig. 9A, B). In contrast, type I commissural neurons were morphologically altered in APP23 mice compared to wild-type mice at 5, 11, and 15 months of age (Fig. 9C, D). In APP23 mice, the apical dendrite was shorter than in wild-type animals (Fig. 9C, D). The basal dendrites exhibited a non-symmetric pattern, short secondary or tertiary branches and their diameter was often reduced (Fig. 9D). In comparison, in wild-type mice this type of neurons showed a symmetrical architecture of the basal dendrites and secondary and tertiary branches were longer than in APP23 transgenic mice (Fig 9C, D). Altered type I commissural neurons in APP23 mice were often located distant from Aβ-plaques identified by subsequent immunostaining with anti-$A\beta_{1-42}$ or by Aβ-plaque-induced autofluorescence (Thal et al., 2002b).

There were no apparent differences in the morphological patterns of type II and type III commissural neurons among APP23 and wild-type mice.

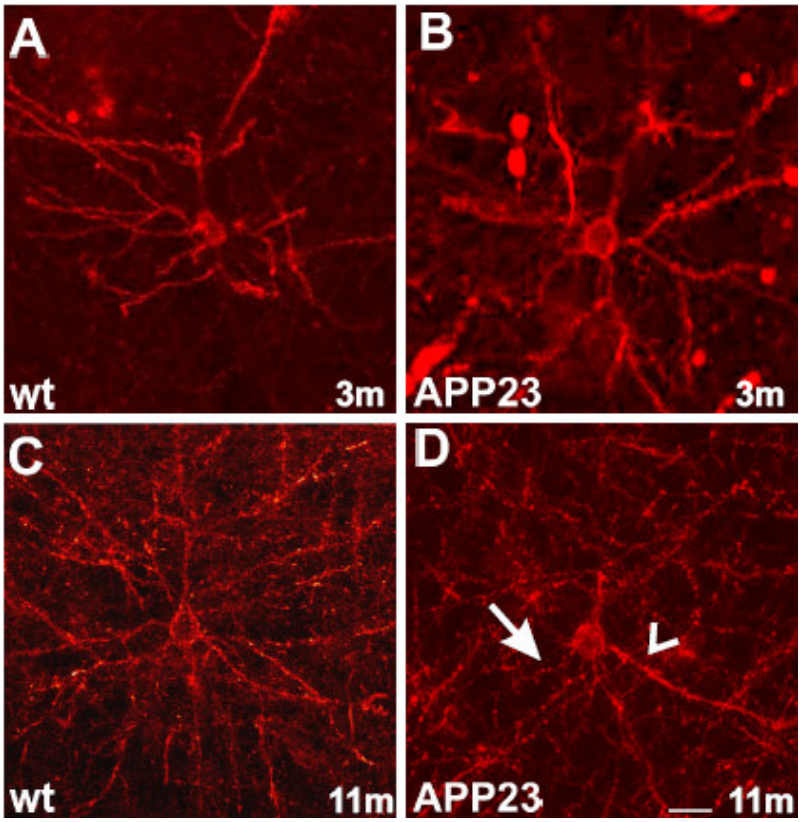

Figure 9: DiI-traced type I commissural neurons in the frontocentral cortex of 3- and 11-month-old wild-type and APP23 mice. **A**: Type I commissural neurons in layer III of the frontocentral cortex show a highly ramified dendritic tree in 3-month-old wild-type mice. The basal dendrites exhibit secondary and tertiary branches and are symmetrically organized. **B**: In APP23 mice of 3 months of age there are no significant differences in the architecture of the dendritic tree when compared to that of wild-type animals. **C**: In 11 months old wild-type animals the dendritic tree of a type I commissural neuron shows further ramifications. The dendritic tree has still a perfect symmetric architecture. **D**: Type I commissural neuron in a 11-month-old APP23 mouse exhibits a dendritic tree that shows a non symmetric architecture of the basal dendrites. A number of basal dendrites are small and shrunken (arrow) while others still appear in regular size (unfilled arrow head). This pattern of type I neurons is strikingly different from that at 3 months of age and that of wild-type animals at 11 months of age. Calibration bar: 22 µm.

4.3. Selective reduction of type I commissural neurons in APP23 mice

Quantitative analysis of traced commissural neurons in 5-15 months of age wild-type mice showed that type II commissural neurons were predominant (60-80%), while type I (10-20%) and type III neurons (10-20%) were less abundant. The number of traced type I neurons appeared to decrease with age but this trend failed significance (trend test: p=0.108) (Fig. 10). In 3-month-old animals a

similar percentage of type I neurons was found (10-20%) while type II neurons were less predominant (40-45%). In these animals the number of type III neurons was higher than in older animals ($p<0.01$; Analysis of variance (ANOVA) corrected for multiple testing by using the Tamhane T2 post hoc-test) and covered 40-45% of all traced commissural neurons (Fig. 10).

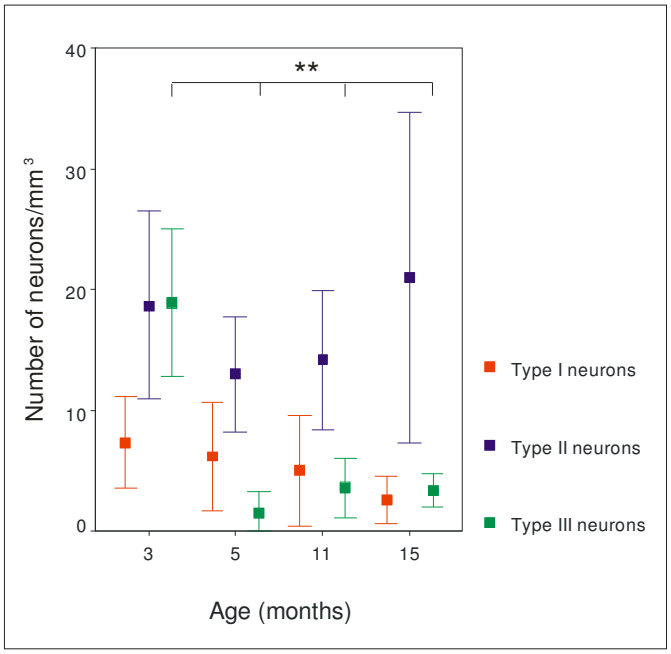

Figure 10. Diagram representing the mean number and standard deviation type I, type II and type III commissural neurons in wild-type mice at 3, 5, 11, and 15 months of age. At 3 months of age, the number of type III neurons/mm^3 was higher than in older animals. In 5-15 months of age wild-type animals, type I and type III commissural neurons were less frequently detectable than type II commissural neurons and represented each 10-20% of the commissural neurons. ** $p<0.01$.

The overall number of commissural neurons did not show significant differences between wild-type and transgenic mice at a given age (Mann-Whitney U-test, corrected for multiple testing: 3 months: $p=0.9917$; 5 months: $p=0.2126$; 11 months: $p=0.9579$; 15 months: $p=0.3232$). However, with increasing expansion of Aβ-deposition throughout the brain the total number of neurons decreased (Poisson regression analysis controlled for age: risk-ratio = 0.967, 95% confidence interval = 0.941 – 0.9938, $p<0.05$; trend-test: $p<0.05$).

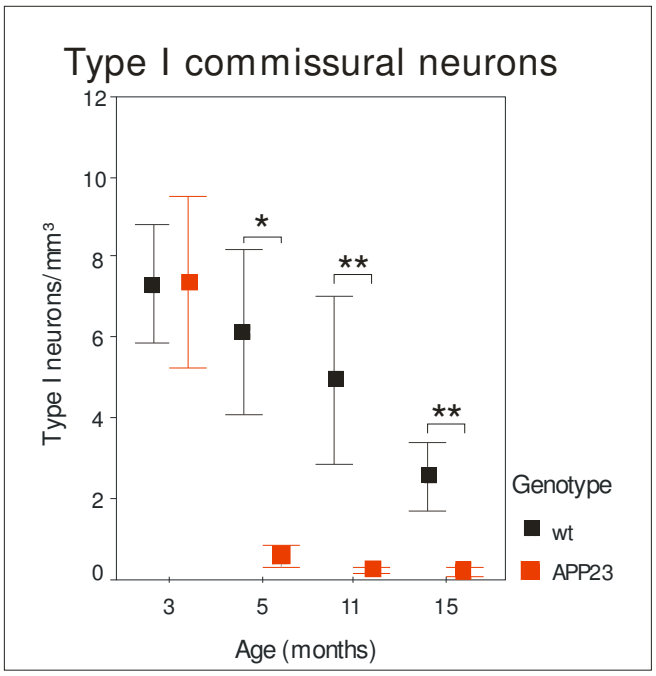

Figure 11: Diagram representing the mean number and standard deviation of type I commissural neurons in wild-type and APP23 mice at 3, 5, 11, and 15 months of age. APP23 mice show a decrease of more than 90% of the type I commissural neurons compared to wild-type mice at 5, 11, and 15 months of age.* p<0.05; ** p<0.01.

In detail, the number of traced type I commissural neurons in APP23 mice was reduced by more than 90% compared to that of wild-type mice at 5, 11 and 15 months of age (Mann-Whitney U-Test, corrected for multiple testing: 5 months APP23 vs. wild-type: $p<0.05$; 11 months APP23 vs. wild-type: $p<0.005$; 15 months APP23 vs. wild-type: $p< 0.01$) but not at 3 months of age (Mann-Whitney *U*-Test, corrected for multiple testing: 3 months APP23 vs. wild-type: $p=0.9917$) (Fig. 11). With the expansion of Aβ-deposition the number of traced type I neurons decreased significantly (Poisson regression analysis controlled for age: risk-ratio = 0.3417, confidence interval = 0.174 – 0.6712, $p<0.005$).

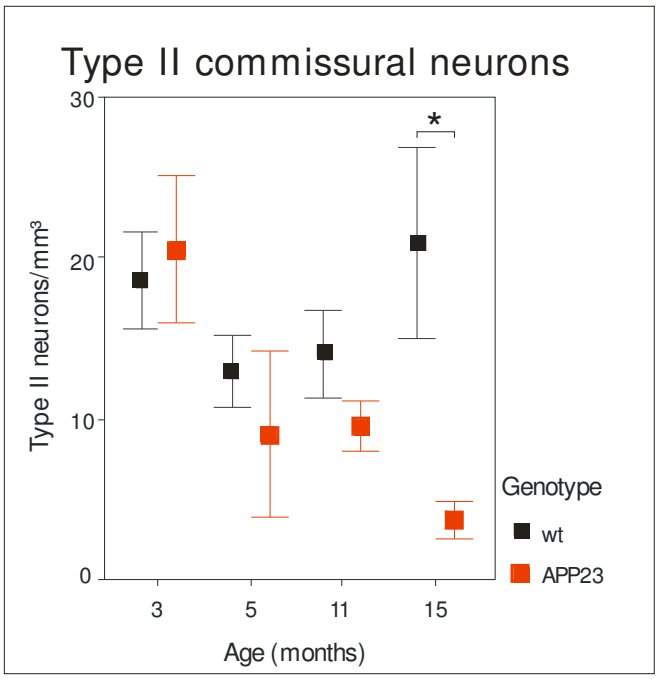

Figure 12: Diagram representing the mean number and standard deviation of type II commissural neurons in each strain at 3, 5, 11, and 15 months of age. There are no significant differences in the number of type II commissural neurons at 3, 5, and 11 months of age between wild-type and APP23 mice. Only in 15-month-old APP23 mice the number of type II commissural neurons is decreased compared to wild-type animals. At this age, less type II neurons are labeled when compared with younger APP23 mice (Kruskal-Wallis H-test: $p<0.005$, trend-test: $p<0.05$). * $p<0.05$; ** $p<0.01$.

The number of type II commissural neurons did not show significant differences between wild-type and APP23 mice at 3, 5 and 11 months of age (Mann-Whitney *U*-Test, corrected for multiple testing: 3 months p=1; 5 months p=0.182; 11 months: p=0.9375) (Fig. 12). However, at 15 months of age a significant reduction of traced type II neurons was observed in APP23 mice compared to wild-type animals (Mann-Whitney *U*-Test, p-values corrected for multiple testing: 15 months: $p< 0.05$). Over all ages, the number of traced type II neurons decreased significantly with the expansion of Aβ-deposition (Poisson regression analysis controlled for age: risk-ratio = 0.9432, confidence interval = 0.9033 – 0.9849, $p<0.01$).

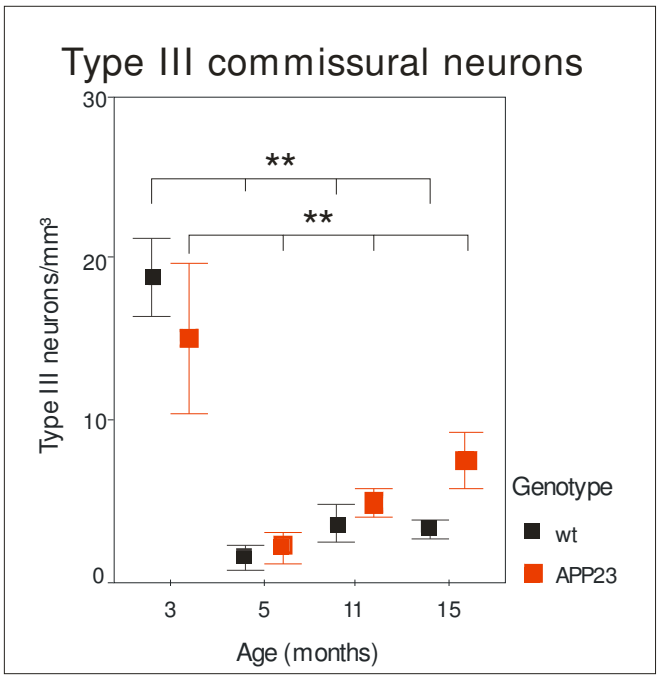

Figure 13: Diagram representing the mean number and standard deviation of type III commissural neurons in each strain at 3, 5, 11, and 15 months of age. Neither at 3 nor at 5, 11, and 15 months of age, there is significant differences in the number of nonpyramidal commissural neurons between wild-type and APP23 mice. Between 3 months of age and 5 - 15 months of age there is a reduction of ~80% of type III neurons.* $p<0.05$; ** $p<0.01$.

The number of type III commissural neurons did not significantly differ among APP23 and wild-type mice neither at 3 nor at 5, 11, or 15 months of age (Mann-Whitney U-Test, corrected for multiple testing: APP23 vs. wild-type: 3 months: p=0,8651; 5 months: p=0.9749; 11 months: p=0.453; 15 months: p=0.3232) (Fig. 13). In addition, there was no significant change in the number of traced type III neurons throughout the phases of Aβ-deposition (Poisson regression analysis controlled for age: risk-ratio = 1.0409, p=0.1533).

4.4. Aβ production in APP23 mice

Western blot analysis confirmed overexpression of human APP and production of $A\beta_{1-40}$ and $A\beta_{1-42}$ in APP23 mice (Fig. 14). Full length APP (flAPP) was detected both in wild-type as well as in APP23 mice. hAPP was detected in APP23 mice at 5 and 11 months of age with the same intensity. However, the levels of $A\beta_{1-40}$ and $A\beta_{1-42}$ clearly increased from 5 to 11 months of age.

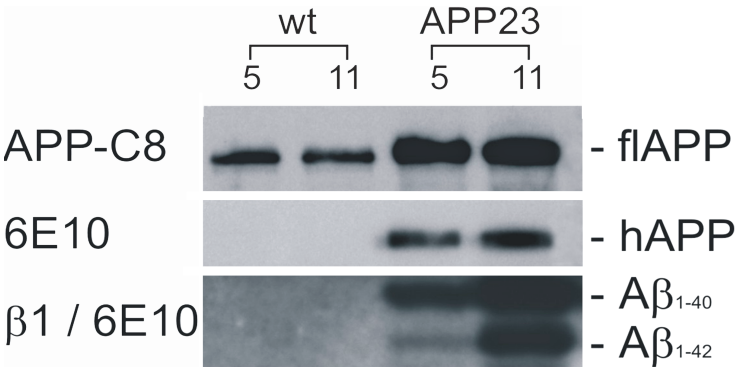

Figure 14: Western blot analysis of APP and Aβ in forebrain homogenates of wild-type and APP23 mice at the ages of 5 and 11 months. Full length APP (flAPP) is detected with an antibody directed against mouse and hAPP (APP-C8). Transgenic hAPP is stained with a human specific Aβ antibody which also reacts with human APP (6E10). In the lowest panel, $A\beta_{1-40}$ and $A\beta_{1-42}$ are detected with the 6E10 antibody after immunoprecipitation with the anti-Aβ antibody β1 except for the 11-month-old APP23 sample. To compensate for the Aβ accumulation, this sample was diluted and represents 80 times less forebrain tissue than the other samples. Both $A\beta_{1-40}$ and $A\beta_{1-42}$ are detectable in APP23 mice at 5 and 11 months of age while no significant amounts of Aβ are seen in wild-type mice.

Quantification of total Aβ levels by ELISA in APP23 mice at 3, 5, 11, and 15 months of age showed a significant exponential increase of Aβ with the age (Tab. 3) (ANOVA corrected for multiple testing by using the Tamhane T2 post hoc-test: $A\beta_{1-40}$ $p<0.001$; $A\beta_{1-42}$ $p<0.001$). Total $A\beta_{1-40}$ levels, thereby, were higher than total $A\beta_{1-42}$ levels (sign test: $p<0.001$). Between 3 and 5 months of age total Aβ levels did not differ significantly (ANOVA corrected for multiple testing by using the Tamhane T2 post hoc-test: $A\beta_{1-40}$ $p=0.786$; $A\beta_{1-42}$ $p=0.963$). However, between 5 and 11 months of age an increase

of both, $A\beta_{1-40}$ and $A\beta_{1-42}$ was seen (ANOVA corrected for multiple testing by using the Tamhane T2 post hoc-test: $A\beta_{1-40}$ $p<0.05$; $A\beta_{1-42}$ $p<0.01$), as well as between 11 and 15 months of age (ANOVA corrected for multiple testing by using the Tamhane T2 post hoc-test: $A\beta_{1-40}$ $p<0.01$; $A\beta_{1-42}$ $p<0.001$).

Table 3: Mean levels of $A\beta_{1-40}$ and $A\beta_{1-42}$ concentration in the forebrain of APP23 mice at 3, 5, 11 and 15 months of age determined by ELISA.

Age (months)	$A\beta_{1-40}$ (pmol/g)	SD		$A\beta_{1-42}$ (pmol/g)	SD	
3	22,51	+/- 3,16		2,25	+/- 0,36	
5	25,94	+/- 5,60	p<0.05	2,46	+/- 0,40	p<0.01
11	5447,09	+/- 1437,67		1668,36	+/-256,46	
15	28919,74	+/- 7699,72	p<0.01	6019,74	+/-1146,88	p<0.001

4.5. Aβ-plaque load in the frontocentral cortex of APP23 mice

Immunohistochemistry with a polyclonal antibody detecting $A\beta_{1-40}$ as well as $A\beta_{1-42}$, revealed no Aβ-deposits in wild-type mice at 3-, 5-, 11-, or 15-month. APP23 mice did not show plaques at 3 months of age (Fig. 15,17A). Single plaques in the frontocentral neocortex were observed in 67% of the APP23 mice at 5 months of age (ANOVA corrected for multiple testing by using the Tamhane T2 post hoc-test: $p<0.05$). However, differences in the Aβ-plaque load did not reach significance between 3- and 5-month-old APP23 mice (ANOVA corrected for multiple testing by using the Tamhane T2 post hoc-test: $p=0.096$) (Fig. 15). Between 5- and 11-month-old APP23 mice the Aβ-plaque load in the frontocentral cortex increased (Fig. 15) (ANOVA corrected for multiple testing by using the Tamhane T2 post hoc-test: $p<0.005$). At 11 months of age all APP23 mice showed Aβ-plaques in the frontocentral cortex. Between the ages of 11 and 15 months there was a further increase in the Aβ-plaque load within the frontocentral cortex (ANOVA corrected for multiple testing by using the Tamhane T2 post hoc-test: $p<0.001$).

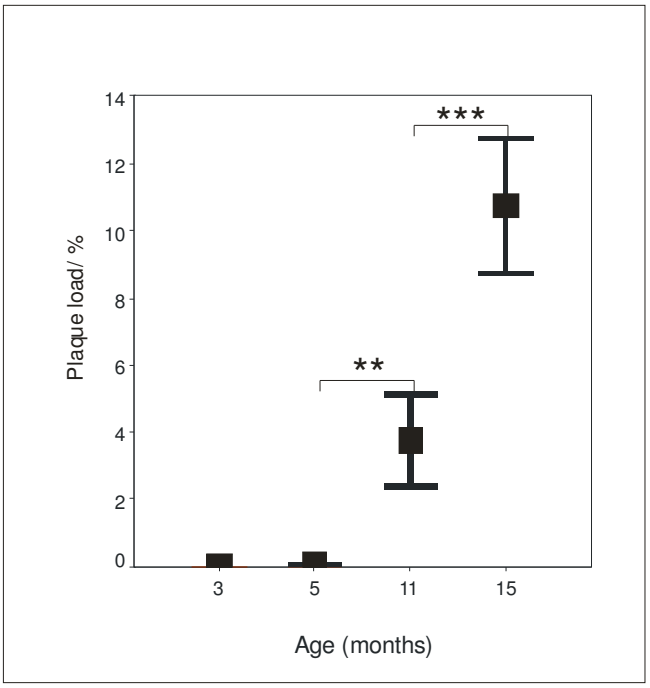

Figure 15: Quantification of the Aβ-plaque load in the frontocentral cortex of APP23 mice. There is no significant difference in the Aβ-plaque load between 3- and 5-month-old animals. The single plaques seen in 5-month-old animals did not lead to a significant increase in the Aβ-plaques load (p=0.096). Between 5 and 11 as well as between 11 and 15 months the Aβ-plaque load increases. Boxes represent mean values. Bars indicate the standard deviation. * p<0.05; ** p<0.01; ***p<0.001.

4.6. Expansion of Aβ-deposition in APP23 mice

Immunohistochemistry with polyclonal antibody detecting $A\beta_{1\text{-}40}$ as well as $A\beta_{1\text{-}42}$ showed the first Aβ-deposits in APP23 mice at 5 months of age (Fig. 16B). Single plaques in the frontocentral cortex were observed in 67% of the APP23 mice representing the phase 1 of Aβ-deposition as it was mention before (see 4.5) (Tab. 4) (ANOVA corrected for multiple testing by using the Tamhane T2 post hoc-test: p<0.05). No other brain area showed Aβ-plaques at this age. 11-month-old mice often exhibited an additional involvement of allocortical brain regions, i.e. the hippocampal formation and the cingulate gyrus in Aβ-deposition (Fig. 16C) representing phase 2 of Aβ-deposition (Fig. 17, Tab.

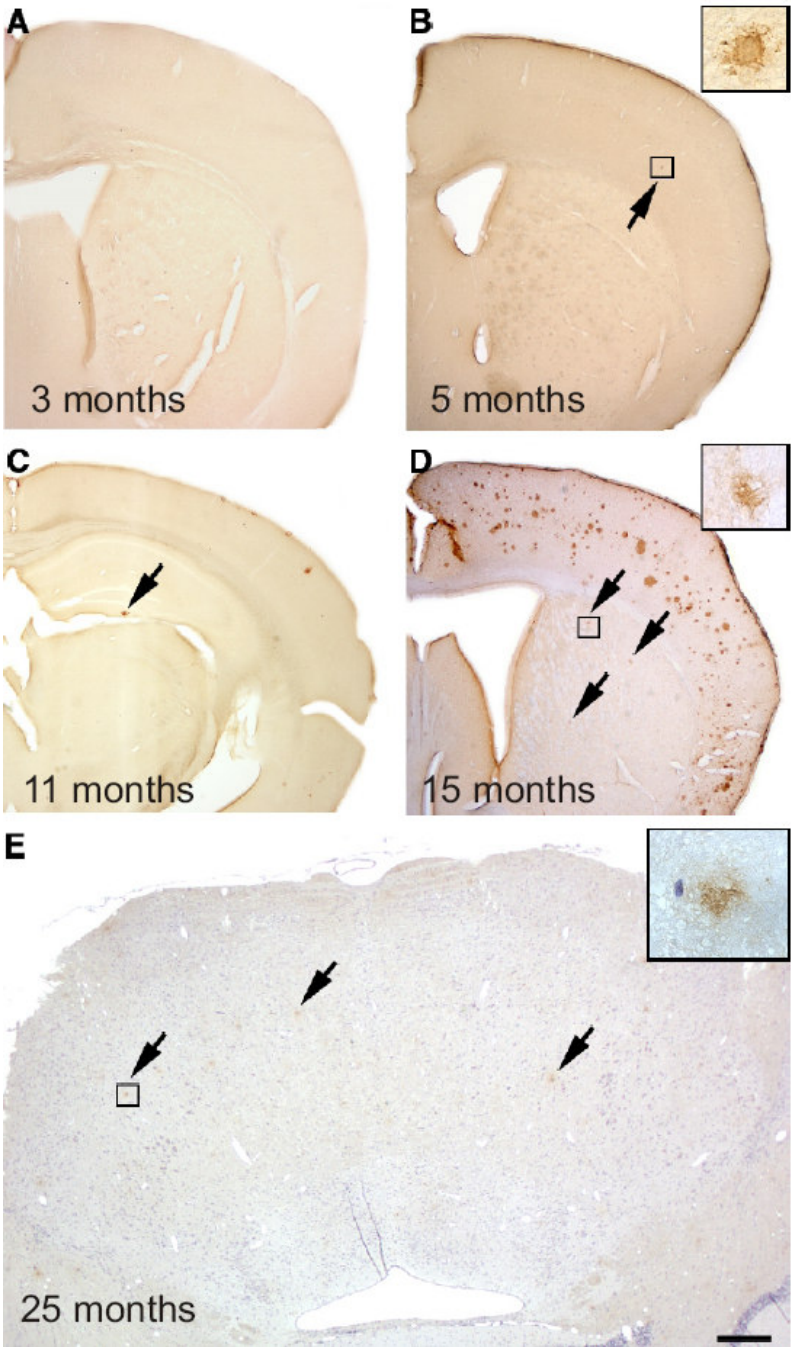

Figure 16. Aβ-deposition in APP-transgenic mice expands into additional brain regions with increasing age. **A:** 3-month-old APP23 mice do not show Aβ-deposits. **B:** Aβ-deposition begins in female APP23 mice at 5 months of age in the neocortex (boxed area). Here, the first amyloid plaques can be identified (inset). **C:** At 11 months of age, allocortical areas, such as the hippocampus, exhibit Aβ-plaques (arrow) in addition to neocortical areas. However, the basal ganglia as well as the thalamus do not show plaques at this stage. **D:** Fifteen-month old female APP23 mice form Aβ plaques in the basal ganglia (striatum; arrows, boxed area). **E:** Aβ deposits in the brain stem occur in mice at 25 months of age (arrows, boxed area). The inset indicates the diffuse nature of these plaques. Calibration bar: **A-D**: 730 µm, **insets B, D, E**: 25 µm.

4) (ANOVA corrected for multiple testing by using the Tamhane T2 post hoc-test: $p<0.005$). Between 11 and 15 months of age an additional Aβ-plaques occurred in the basal ganglia as well as in the thalamus (Fig. 16D) indicating phase 3 of Aβ-deposition (ANOVA corrected for multiple testing by using the Tamhane T2 post hoc-test: $p<0.001$) (Fig. 17, Tab. 4).

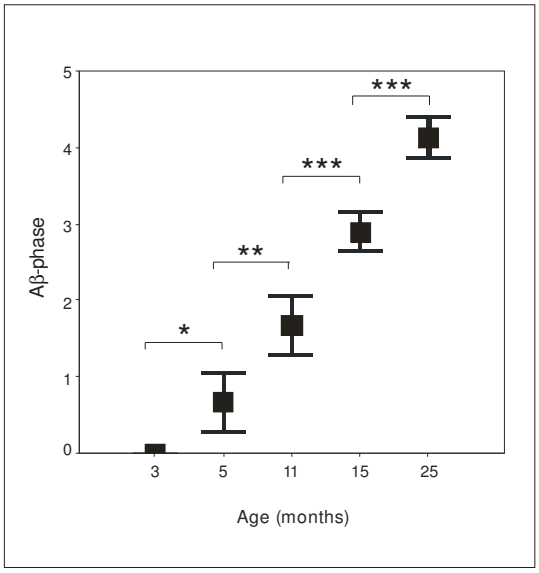

Figure 17: Distribution of Aβ-plaques as described by the phases of Aβ-deposition (Thal et al., 2002a) in APP23 mice. 3-month-old animals do not show plaques. Aβ-deposition starts with the first plaques in 5-month-old APP23 mice. 67% of these mice exhibited Aβ-plaques in a distribution pattern related to phase 1. A significant expansion of Aβ-deposition as represented by an increasing phase is seen with advancing age. Boxes represent mean values. Bars indicate the standard deviation. * $p<0.05$; ** $p<0.01$; ***$p<0.001$.

To confirm that Aβ-deposition in APP23 mice follows the same hierarchical involvement of different regions as in human brain (Thal et al., 2002a), additional paraffin sections from 25-month-old APP23 mice were included for the staging study. At 25 months of age, 75% of the APP23 mice showed additional Aβ-deposits in the midbrain representing phase 4 of Aβ-deposition (Fig. 16E) and 18,2% of the mice showed an involvement of the pons representing phase 5 of Aβ-deposition (Fig. 17, Tab. 4) (ANOVA corrected for multiple testing by using the Tamhane T2 post hoc-test: $p<0.001$). Aβ-

deposits in APP23 mice exhibited equal staining patterns with anti-$A\beta_{42}$ and anti-$A\beta_{40}$ antibodies at all ages.

Table 4. Percentage of mice exhibiting Aβ-deposits in a given phase at a given age.

Age (months)	Phase 0	Phase 1	Phase 2	Phase 3	Phase 4	Phase 5
3	100,0%	0,0%	0,0%	0,0%	0,0%	0,0%
5	33,3%	66,7%	0,0%	0,0%	0,0%	0,0%
11	0,0%	33,3%	66,7%	0,0%	0,0%	0,0%
15	0,0%	0,0%	11,1%	88,9%	0,0%	0,0%
26	0,0%	0,0%	0,0%	6,3%	75,0%	18,2%

4.7. Axonal sprouting of commissural neurons in APP23 mice

Immunohistochemistry with antibodies directed against APP and GAP43 showed the presence of immunolabeled, thickened axon endings in the frontocentral cortex of 3-month-old wild-type and APP23 mice indicative for axonal sprouting (Fig. 18A-D). In the DiI-traced sections we found collateral sprouting in wild-type and APP23 mice at 3 months of age. Single axons of commissural neurons with growth cones were seen in layers II and III of the frontocentral cortex of the DiI-traced sections (Fig. 18E). In 5-month-old mice thickened axon endings of commissural neurons in DiI-traced sections were no longer observed. However, single APP and GAP43-positive, thickened axon endings were found in APP23 mice but not in wild-type mice at this age (Fig. 18F-I).

Sprouting of commissural neurons around plaques was observed in 11- and 15-month-old APP23 mice in DiI-traced sections (Fig. 19C) as well as in APP and GAP43-stained sections (Fig. 19A, B). Wild-type mice did not show sprouting of commissural neurons in this age in DiI-traced sections. Only single APP and GAP43-positive sprouting axons were detected in the frontocentral cortex of 15-month-old wild-type mice.

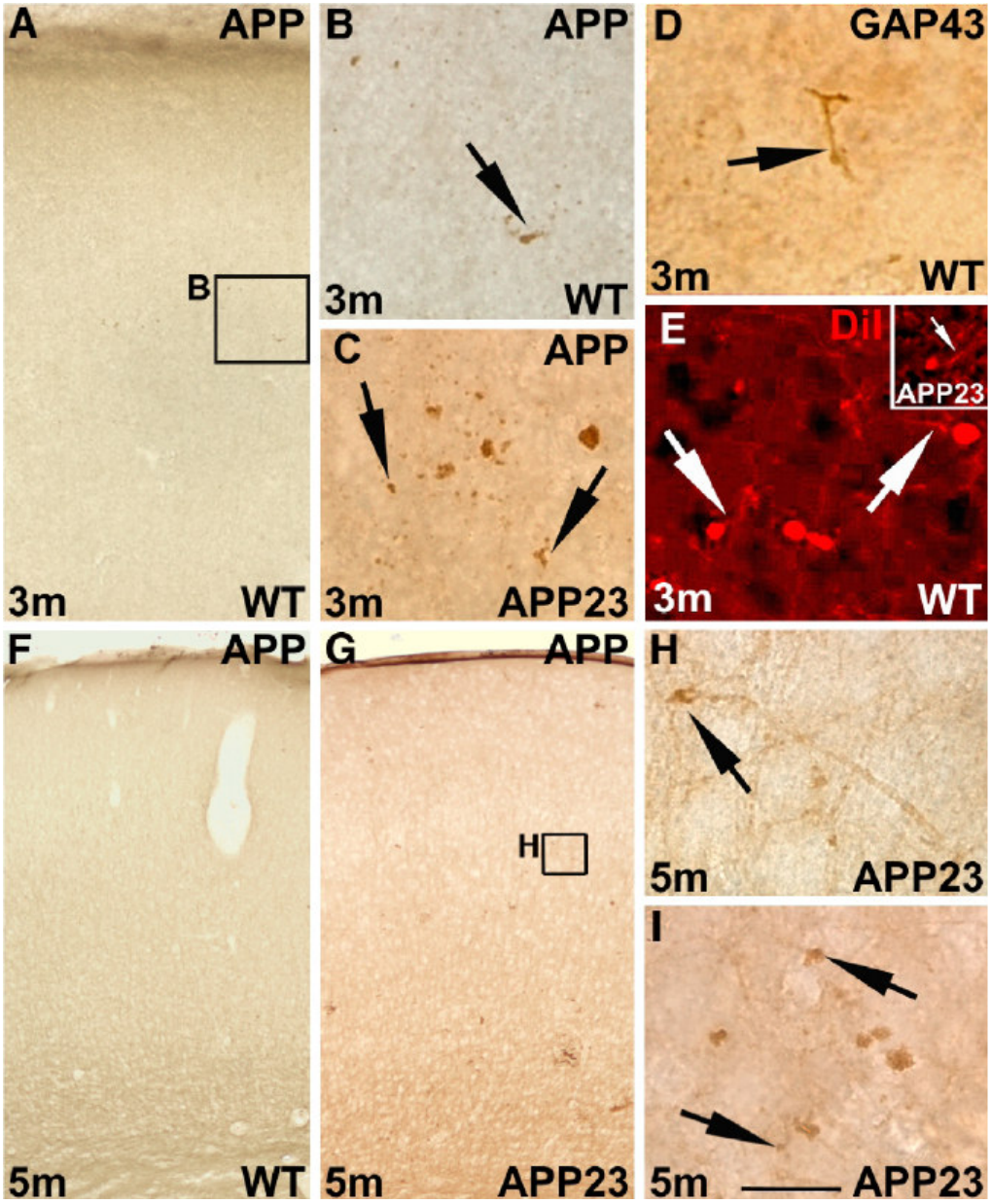

Figure 18: Sprouting and degenerating axons in the frontocentral cortex of wild-type (wt) and APP23 mice. **A-E**: APP and GAP43-positive thickened axonal endings in the frontocentral neocortex of wild-type and APP23 mice at 3 months of age. APP positive axonal endings (arrow in **B**) are found in layer III of the frontocentral cortex (**A, B** representing the enlargement of the boxed area in **A**). The axonal endings occur in wild-type as well as in APP23 mice and appear as thickened growth cones of sprouting axons (arrows in **B, C**) also exhibiting GAP43 (arrow in **D**). DiI-tracing also shows swollen axon endings (arrows) in layer III of the contralateral hemisphere indicating an involvement of commissural neurons in these changes (**E**). **F-I**: At 5 months of age wild-type mice do not show APP or GAP43 positive sprouting or degenerating axons (**F**). In contrast, APP23 mice exhibit single APP positive, thickened axonal endings (arrows in **H-I; H** represents the enlargement of the boxed area in **G**). Calibration bar: **A, F, G**: 300 µm, **B-E, H, I**: 20 µm.

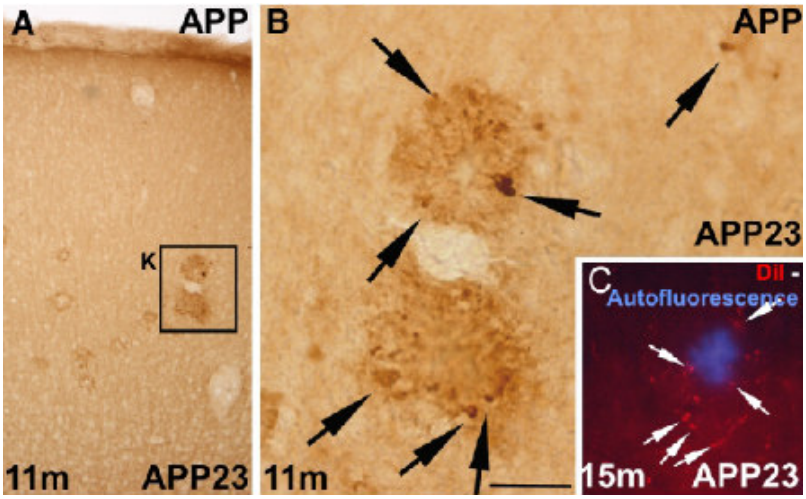

Figure 19. At 11 and 15 months of age APP positive dystrophic neurites are seen in association with plaques (arrows in **B** representing the enlargement of the boxed area in **A**). Some of these neurites were identified as aberrant sprouting axons (arrows) arising from commissural neurons by DiI-tracing around amyloid plaques in the contralateral frontocentral cortex (**C**). The amyloid nature of the plaque is demonstrated by the exhibition of the Aβ-plaque specific blue autofluorescence under UV-light excitation (Thal et al., 2002b). Calibration bar: **A**: 300 µm. **B**: 40 µm, **C**: 70 µm.

5. DISCUSSION

In this study, it is shown that three types of commissural neurons in layer III of the mouse frontocentral cortex can be identified using tracing methods. These different neuron types are hierarchically affected by Aβ-induced neurodegeneration. The deposition of the first Aβ-plaques is, thereby, associated with the onset of neurodegeneration in APP23 mice. Expansion of Aβ-deposition into further brain regions goes along with increasing age and the involvement of a second type of commissural neurons in neurodegeneration and confirms that the step-by-step expansion of Aβ-deposits in the brain represents the time course of Aβ-deposition. The complexity of the dendritic morphology is, thereby, related to the vulnerability of these different types of neurons.

5.1. Types of commissural neurons in the frontocentral cortex of the mouse brain

This study confirms and extends previous reports that describe different types of pyramidal and non-pyramidal neurons projecting through the corpus callosum (Hughes and Peters, 1992; Martinez-Garcia et al., 1994). The distinction of the three types of commissural neurons in the mouse frontocentral cortex is based on their morphological appearance after retrograde tracing with DiI. It is confirmed by using biotinylated dextrane in vivo tracing as an additional method.

Type I commissural neurons are characterized by a pyramidally shaped perikaryon and apical and basal dendrites with a heavily ramified and spiny dendritic tree within layer II-III. Type II commissural neurons represent neurons with a pyramidally shaped perikaryon and apical and basal dendrites, which do not show extensive further ramifications in layer III in a given tissue section. However, 3D-reconstruction revealed that the basal dendrites of these neurons start branching distant

from the perikaryon. Type III commissural neurons are non-pyramidal neurons and have a circular cell body with a few tiny dendrites.

In contrast to the other types of commissural neurons, type III neurons are reduced in number in 5-, 11- and 15-month-old animals in comparison to 3-month-old mice regardless of the genotype. Thus, an effect of Aβ or APP-overexpression is not responsible for the reduction of type III neurons because wild-type mice show the same effects as APP23 mice. To explain this finding further studies are required. Developmental or maturation-related phenomena (Fritzsch et al., 1997) might be involved.

All three types of neurons were found in all mice studied and their axons projected through the corpus callosum to the contralateral hemisphere. Since tracer-labeled type I, type II, and type III commissural neurons were visible in the same section close to one another and type II neurons showed dendritic ramification in the molecular layer it seems unlikely that DiI tracing of neurons without a ramified dendritic tree is due to dysfunctional tracing rather than to the exhibition of specific morphological types of neurons. Galuske and Singer (Galuske and Singer, 1996) also reported that once a given neuron is stained with DiI all cell processes will be labeled. Moreover, a second tracing method based on in vivo transport of the biotinylated dextrane (Reiner et al., 2000) confirmed the presence of three different types of commissural neurons.

The heterogeneous morphological pattern of commissural neurons in the frontocentral cortex of mice confirms and extends the finding of other authors that the visual cortex contains different types of callosal commissural neurons (Voigt et al., 1988; Buhl and Singer, 1989; Martinez-Garcia et al., 1994). They also reported the presence of commissural neurons of pyramidal and non-pyramidal types. Cortical commissural neurons project to different layers of the contralateral hemisphere (Wise and Jones, 1976; Martinez-Garcia et al., 1994). Therefore, the different types of frontocentral commissural neurons may terminate in different layers of the contralateral hemisphere and may have specific functions in commissural information processing.

5.2. Degeneration of commissural neurons in APP23 mice

Two of the three types of commissural neurons were reduced in number when traced in APP23 transgenic mice. Type I commissural neurons were significantly reduced in number in APP23 mice beginning at 5 months of age. The surviving type I commissural neurons in these mice exhibited alterations of the dendritic tree in comparison to wild-type animals. The other types of commissural neurons did not show obvious differences between transgenic and wild-type mouse lines at this point in time. The second type of neurons showing degenerative changes, type II commissural neurons, was reduced in number at 15 months of age. With increasing age, Aβ-plaque load, and Aβ-expansion the second type of neurons became involved in Aβ-induced neurodegeneration. However, type III commissural neurons were not altered.

The degeneration of type I and type II commissural neurons in APP23 mice can be interpreted 1) as a result of selective neuronal death, 2) as the result of dendritic alterations, or 3) as a consequence of axonal damage (Fig. 20). The first possibility of selective neuronal death is supported by the decrease of the total number of neurons in the hippocampus of APP transgenic mice indicating that neuronal loss can result from abnormal production of Aβ (Fig. 20B) (Calhoun et al., 1998; Schmitz et al., 2004). A second supporting argument is that in Down syndrome patients overexpressing APP (Neve et al., 1988) neuronal loss is accentuated in layer III of the frontocentral cortex (Davidoff, 1928). On the other hand, the second possibility that the reduction of the heavily ramified type of commissural neurons is due to dendritic changes is supported by a recent finding indicating that dendritic length is reduced in a specific group of dentate granule cells in PDAPP transgenic mice (Fig. 20C) (Wu et al., 2004). Together with our finding of an asymmetrically ramified dendritic tree in altered type I commissural neurons it is likely that dendritic alterations would at least precede neuronal death. In so doing, it is possible that degenerated type I and type II neurons may appear morphologically as type II or type III commissural neurons, respectively. The third hypothesis for the

reduction of the number of traced commissural neurons is a loss of axonal connectivity between the hemispheres (Fig. 20D). This hypothesis is supported by axonal sprouting seen in aged APP-transgenic mice (Phinney et al., 1999; Teter and Ashford, 2002) indicating regeneration after axonal injury (Deller and Jucker, 2001) and by the degeneration of myelinated axons (Bartzokis et al., 2003), especially in the corpus callosum of human AD-cases (Weis et al., 1991; Yamauchi et al., 1993; Hampel et al., 1998). However, our tracing study as well as that of Phinney et al. (Phinney et al., 1999) did not exhibit collateral sprouting of commissural neurons in 5-month-old APP23 mice already exhibiting a decrease in the number of traced type I commissural neurons. Abnormal axonal sprouting of commissural neurons in APP23 mice starts at 11 months of age and, therefore, axonal damage may not be the first step in the degeneration of these neurons.

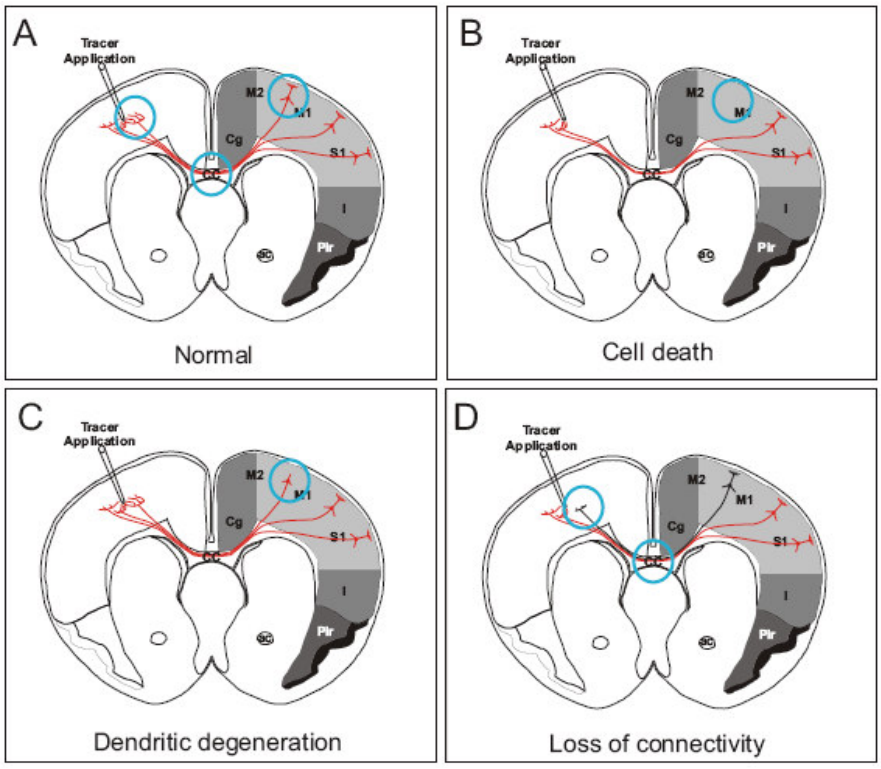

Figure 20. Possible interpretations for the reduction of traced commissural neurons represented in a coronal section of mouse brain at the frontocentral level. The schematic representation shows commissural neurons (red) with axonal terminals in contact with the area where the tracer was applied. Blue circles are located in the areas potentially involved in the degeneration of these commissural neurons. Figure **A** shows no neuronal damage. **B**: One explanation for the reduced number of traced neurons the death of these neurons. **C**: Dendritic alterations may also explain the degeneration of these neurons. **D**: Loss of connectivity due to axonal damage, may lead to a reduction of traced commissural neurons although the cell soma of the neurons is still alive. In this event one would expect collateral sprouting.

Single APP and GAP-43 positive neurites occur in the frontocentral cortex of APP23 mice at 5-month indicative for axonal sprouting (Masliah et al., 1992a; Masliah et al., 1992b). Since commissural neurons do not show sprouting at this age, these APP and GAP-43 positive neurites represent sprouting axon terminals from non-commissural neurons. Such a sprouting is not seen in wild-type littermates. Aβ aggregates alone do not explain this selective sprouting. If Aβ aggregates alone would induce such a sprouting one would expect a contribution of neurites from all types of afferent neurons including commissural neurons. Therefore, it is tempting to speculate that these sprouting neurites in 5-months-old APP23 mice represent reactive sprouting following the degeneration of type I commissural neurons.

Taken together, dendritic and axonal degeneration as well as neuronal death may be involved in the degeneration of type I and type II commissural neurons in a distinct sequence. In a first step dendritic processes of the nerve cells may degenerate presumably followed by axonal damage and, finally, nerve cell death. This sequence is similar to that seen in human AD for neurons accumulating NFTs (Bancher et al., 1989; Braak et al., 1994; Thal et al., 2000a). Here, neurodegeneration starts with dendritic and perikaryal accumulation of abnormal τ-protein, followed by the creation of NFTs, axonal accumulation of abnormal τ-protein in the target region of affected neurons and finally, neuronal death (Braak et al., 1994; Sassin et al., 2000; Thal et al., 2000a).

5.3. Aβ-deposition in APP23 mice

In AD brain, different brain regions become involved in a distinct hierarchical sequence in β-amyloidosis and NFT generation (Braak and Braak, 1991; Thal et al., 2002a). The evolution of Aβ-deposition in APP23 mice follows the same sequence as in the human brain (Wiederhold et al., 2004; Thal et al., 2006a). The first phase shows only neocortical deposits. Additional involvement of allocortical regions characterized phase 2. In the third phase additional Aβ deposits were found in the

basal ganglia and the diecephalon whereas the midbrain and the lower brain stem nuclei become involved in phase 4. In the 5th and final phase Aβ-deposition also occurred in the pons and the cerebellum. In APP23 mice Aβ-deposition started with phase 1 at 5 months of age and then expanded with advancing age until 25 months of age.

In so doing, the phases of Aβ-deposition in mice represent the time course of β-amyloidosis. The similar sequence of Aβ-deposition in the human brains suggests that this sequence represents the time course of AD-related pathology in the human brain.

5.4. The relation between neurodegeneration and Aβ-pathology

The loss of traceable type I commissural neurons in 5-month-old APP23 mice is associated with the deposition of the first Aβ-plaques within the frontal cortex of these animals. However, total Aβ-levels as well as the Aβ-plaque load did not differ significantly between 3 and 5 months old APP23 mice and there was no close spatial relationship between Aβ-plaques and degenerating commissural neurons in 5-month-old APP23 mice. This result indicates that Aβ-induced degeneration of neurons in the brain is not due to a simple increase in Aβ-levels or to Aβ-plaques themselves but due to qualitative changes in the status of Aβ-aggregation. Insofar, our results support other studies that the aggregation of Aβ to soluble Aβ-oligomers and/or fibrils is required for Aβ-toxicity (Podlisny et al., 1995; Kayed et al., 2003; Kim et al., 2003; Cleary et al., 2005) and go beyond the findings of other authors that Aβ-plaques induce local dendritic or neuritic degeneration (Tsai et al., 2004; Brendza et al., 2005; Spires et al., 2005).

The finding of a hierarchical involvement of different types of neurons in Aβ-induced neurodegeneration further extents the present knowledge of Aβ-toxicity and argues in favor of a selective vulnerability of neurons to Aβ. Since this study is done in commissural neurons projecting

into the same area of the contralateral cortex, all neurons have the same axon lengths and all neurons function as commissural neurons. Axon lengths and the function of the neuron do, therefore, not appear to be responsible for the selective vulnerability of distinct types of neurons. All pyramidal neurons use excitatory amino acids (glutamate or aspartate) as transmitter (Conti et al., 1988; Giuffrida and Rustioni, 1989). Thus, at least type I and type II commissural neurons share a similar neurotransmitter but differ in their vulnerability. Therefore, the selective vulnerability of commissural neurons is most likely not due to the neurotransmitter of the different types of commissural neurons examined in this study.

The most significant difference between type I, type II, and type III commissural neurons is the morphology of the dendritic tree (Fig. 21). Type I neurons exhibit a highly ramified dendritic tree with basal dendrites branching exclusively in layer III whereas type II neurons have a less ramified dendritic tree with dendrites also branching into layer IV. The type III neurons, in contrast, show only single dendrites without significant further ramification into secondary and tertiary dendrites. Thus, it is tempting to speculate that neurons with a highly ramified dendritic tree present a better target for toxic changes by oligomeric and/or fibrillar Aβ than neurons with a less ramified dendritic tree. This hypothesis is supported 1) by the finding of Roselli et al. (Roselli et al., 2005) that soluble Aβ-oligomers induce NMDA-dependent degradation of postsynaptic density-95 protein at glutamatergic synapses on dendrites, 2) by the Aβ-induced inhibition of long-term potentiation (Wang et al., 2002), and 3) by the loss of dendritic spines seen in the vicinity of amyloid plaques (Tsai et al., 2004; Spires et al., 2005). Our finding that Aβ-induced neurotoxicity induces dendritic alterations of type I commissural neurons also argues in favor of the dendritic tree to be the primary target of Aβ-toxicity. The primary deposition of Aβ in the neocortical layers III and V (Braak and Braak, 1991b; Price et al., 1991; Arriagada et al., 1992; Thal et al., 2000b) may support this hypothesis insofar as neurons with a dendritic tree branching exclusively within layer III and the molecular layer are target of Aβ-induced

neurodegeneration at an earlier point in time compared to neurons with basal dendrites escaping layer III by branching into layer IV.

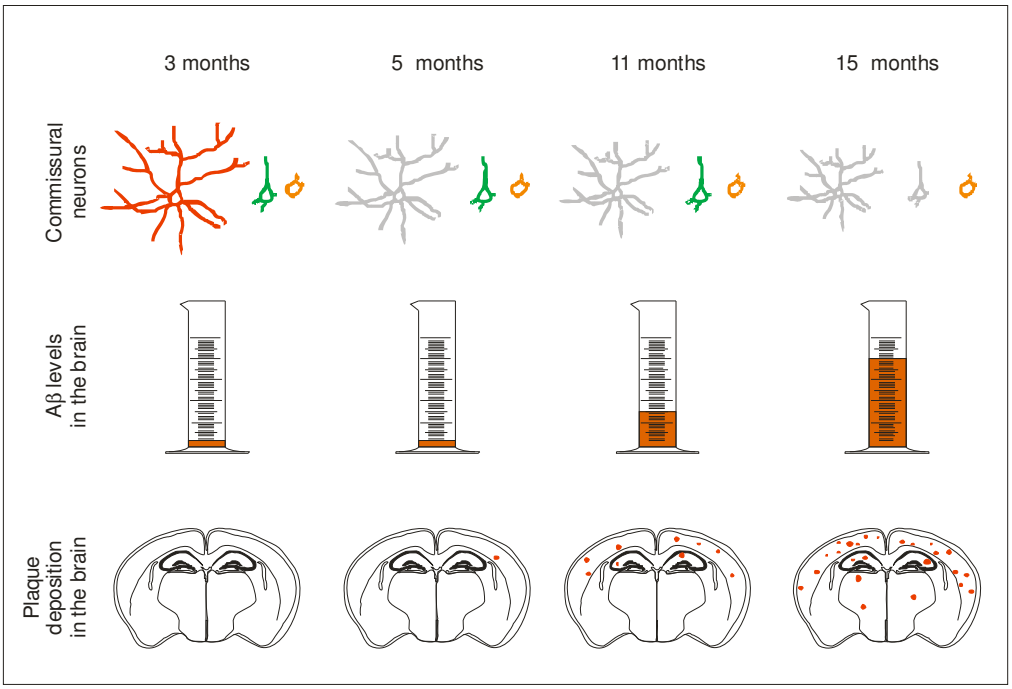

Figure 21: Neurodegeneration in APP23 mice begins when Aβ aggregates can be detected as plaques for the first time at 5 months of age. Degeneration of neurons is represented in the figure by changing the color of the neurons to gray. The Aβ-level in the brain is not responsible for neurodegeneration at 5 months of age because 3- and 5-month-old APP23 mice have similar Aβ-levels but only mice at 5 months of age show neurodegeneration. There is selective vulnerability for Aβ-induced neurodegeneration of distinct types of commissural neurons. The type I commissural neurons (red) are most vulnerable to Aβ whereas type III neurons (orange) are not vulnerable and type II neurons (green) are significantly less vulnerable than type I neurons. The selective vulnerability against Aβ is related to the anatomy of the dendritic tree. Those neurons with the most ramified dendritic tree (type I commissural neurons marked in red) degenerate first. Those neurons with an almost negligible dendritic tree (type III commissural neurons marked in orange) do not degenerate while neurons with a moderately ramified dendritic tree (type II commissural neurons marked in green) degenerate when high levels of Aβ are present in the brain.

These results in concert with that of other authors (Wang et al., 2002; Roselli et al., 2005) support the hypothesis that oligomeric and/or fibrillar Aβ-aggregates interact with dendrites and that neurons may degenerate when their dendrites are exposed to Aβ-aggregates. The size of the target for Aβ, i.e. the dendritic tree surface in a given area, presumably contributes to the vulnerability of

neurons to Aβ. The primary involvement of dendrites in Aβ-toxicity has also been demonstrated in dentate gyrus neurons (Wu et al., 2004). The interaction of ADDLs with the dendrites (Lacor et al., 2004) could explain why Wu et al. (Wu et al., 2004) did not detect any Aβ-deposits although they found dendritic degeneration and it could also explain why 33 % of the 5 months old APP23 mice in our study did show neurodegeneration in the absence of Aβ-deposits. Moreover, it is highly unlikely that the principle function of a neuron (e.g., the function as a commissural neuron), the lengths of its axon, and the neurotransmitter used are the only factors determining selective vulnerability against Aβ. Our results show that theories of selective vulnerability in AD based upon the principal function and axon length of neurons (Braak et al., 2000) need to be supplemented by other factors to explain Aβ-induced selective vulnerability. The morphology of the dendritic arbor presumably contributes to this selective vulnerability of neurons against Aβ as demonstrated here.

5.5. The impact of Aβ-induced progressive neurodegeneration for AD

Aβ alters different types of neurons in a distinct hierarchical sequence in an animal model for Aβ-pathology. After the onset of the degeneration of a distinct type of neurons a further type of neurons became involved with increasing Aβ-pathology. Other studies showing degeneration of different types of neurons in animal models for AD used double or triple transgenic mice (Lewis et al., 2001; Oddo et al., 2003b; Schmitz et al., 2004). In these animals neurodegeneration cannot be addressed exclusively to Aβ because presenilin 1 (Oddo et al., 2003b; Schmitz et al., 2004) and/ or mutant τ-protein (Lewis et al., 2001; Oddo et al., 2003b) are co-expressed. In contrast, single APP-transgenic mice used in this study allow the conclusion that Aβ alone is capable of inducing progressive neurodegeneration. Since humans show a hierarchical sequence in which different types of neurons develop AD-related neurofibrillary tangles and neuronal loss (Braak and Braak, 1991b) which

parallels the step-by-step expansion of Aβ-deposits into further brain regions (Thal et al., 2002a) similar to neurodegeneration and Aβ-deposition in mice these results suggest that Aβ is capable of inducing progressive neurodegeneration in AD. Therefore, these results support Aβ to be a major therapeutic target for AD treatment preferentially in pre-clinical stages to prevent progression of Aβ-induced neurodegeneration. However, since Aβ supports progression of neurodegeneration Aβ-lowering treatment strategies may also be helpful in later stages to stop the disease progression.

5.6. Future perspectives

The association between the expansion of Aβ pathology with cognitive decline in AD patients suggests that therapies aimed at lowering the production of Aβ might be beneficial. Passive as well as active immunization of APP-transgenic mice with anti-Aβ antibodies reduces the Aβ-load in the brain and improves the performance in cognition tests for mice (Schenk et al., 1999; Janus et al., 2000; Morgan et al., 2000). However, the first human patient died after Aβ-immunotherapy still showed severe neuronal pathology although the Aβ-load was lower than in untreated AD cases (Nicoll et al., 2003). Therefore, the question arises whether the reduction of Aβ-deposits enables protection from neurodegeneration and/or allows recovery of degenerated neurons. Type I commissural neurons in APP23-transgenic mice are an ideal target to address this question. In the event that immunization after the onset of neurodegeneration in APP23 mice leads to a recovery of type I commissural neurons, it would indicate that Aβ-induced neurodegeneration is reversible as long as the neurons do not die. On the other hand, if Aβ-induced nerve cell damage is not reversible but immunization can be prevented when applied prior to the onset of degeneration, Aβ-lowering treatment strategies could stop the disease progression. Thus, the impact of Aβ-immunotherapy on vulnerable neurons such as the Type I commissural neurons will allow the determination of the most favorable therapeutic management for

Aβ-lowering therapies in the animal model and, in so doing, help to optimize its future clinical application in AD treatment.

6. CONCLUSIONS

1) The expansion of Aβ-deposition into further brain regions as reported in the human brain represents the time course of the development of β-amyloidosis in the brain as seen in the mouse model.

2) Aggregated forms of Aβ induce degeneration of commissural pyramidal neurons in the frontocentral cortex as soon as plaque deposition starts.

3) Aβ-protein induces selective neurodegeneration in a distinct hierarchical sequence.

4) The involvement of additional neuronal subpopulation is associated with the increase of Aβ levels and with the expansion of Aβ-deposition into further brain regions.

5) Therefore, these results strongly support the hypothesis that Aβ itself is capable of inducing progressive neurodegeneration in AD as demonstrated in APP transgenic mice.

7. REFERENCES

Alzheimer A (1907) Ueber eine eigenartige Erkrankung der Hirnrinde. Allg Zschr Psych 64:146-148.

Andra K, Abramowski D, Duke M, Probst A, Wiederhold KH, Burki K, Goedert M, Sommer B, Staufenbiel M (1996) Expression of APP in transgenic mice: a comparison of neuron-specific promoters. Neurobiol Aging 17:183-190.

Arnold SE, Hyman BT, Flory J, Damasio AR, Van Hoesen GW (1991) The topographical and neuroanatomical distribution of neurofibrillary tangles and neuritic plaques in the cerebral cortex of patients with Alzheimer's disease. Cereb Cortex 1:103-116.

Arriagada PV, Marzloff K, Hyman BT (1992) Distribution of Alzheimer-type pathologic changes in nondemented elderly individuals matches the pattern in Alzheimer's disease. Neurology 42:1681-1688.

Baker GE, Reese BE (1993) Using confocal laser scanning microscopy to investigate the organization and development of neuronal projections labeled with DiI. Methods Cell Biol 38:325-344.

Ball MJ (1977) Neuronal loss, neurofibrillary tangles and granulovacuolar degeneration in the hippocampus with ageing and dementia. A quantitative study. Acta Neuropathol (Berl) 37:111-118.

Bancher C, Braak H, Fischer P, Jellinger KA (1993) Neuropathological staging of Alzheimer lesions and intellectual status in Alzheimer's and Parkinson's disease patients. Neurosci Lett 162:179-182.

Bancher C, Brunner C, Lassmann H, Budka H, Jellinger K, Seitelberger F, Grundke-Iqbal I, Iqbal K, Wisniewski HM (1989) Tau and ubiquitin immunoreactivity at different stages of formation of Alzheimer neurofibrillary tangles. Prog Clin Biol Res 317:837-848.

Bartzokis G, Cummings JL, Sultzer D, Henderson VW, Nuechterlein KH, Mintz J (2003) White matter structural integrity in healthy aging adults and patients with Alzheimer disease: a magnetic resonance imaging study. Arch Neurol 60:393-398.

Bertram L, Tanzi R (2003) Genetics of Alzheimer's disease. In: Neurodegeneration: The molecular pathology of dementia (Dickson D, ed), pp 40-46. Basel: ISN Neuropath Press.

Blocq P, Marinesco G (1892) Sur les lesions et la pathologenie de l'epilepsie dite essentielle. Semaine Med 12:445-446.

Braak E, Braak H, Mandelkow EM (1994) A sequence of cytoskeleton changes related to the formation of neurofibrillary tangles and neuropil threads. Acta Neuropathol 87:554-567.

Braak H, Braak E (1991a) Demonstration of amyloid deposits and neurofibrillary changes in whole brain sections. Brain Pathol 1:213-216.

Braak H, Braak E (1991b) Neuropathological stageing of Alzheimer-related changes. Acta Neuropathol 82:239-259.

Braak H, Del Tredici K, Schultz C, Braak E (2000) Vulnerability of select neuronal types to Alzheimer's disease. Ann N Y Acad Sci 924:53-61.

Brendza RP, Bacskai BJ, Cirrito JR, Simmons KA, Skoch JM, Klunk WE, Mathis CA, Bales KR, Paul SM, Hyman BT, Holtzman DM (2005) Anti-Abeta antibody treatment promotes the rapid recovery of amyloid-associated neuritic dystrophy in PDAPP transgenic mice. J Clin Invest 115:428-433.

Buhl EH, Singer W (1989) The callosal projection in cat visual cortex as revealed by a combination of retrograde tracing and intracellular injection. Exp Brain Res 75:470-476.

Calhoun ME, Wiederhold KH, Abramowski D, Phinney AL, Probst A, Sturchler-Pierrat C, Staufenbiel M, Sommer B, Jucker M (1998) Neuron loss in APP transgenic mice. Nature 395:755-756.

Callahan CM, Hall KS, Hui SL, Musick BS, Unverzagt FW, Hendrie HC (1996) Relationship of age, education, and occupation with dementia among a community-based sample of African Americans. Arch Neurol 53:134-140.

Cao X, Sudhof TC (2001) A transcriptionally [correction of transcriptively] active complex of APP with Fe65 and histone acetyltransferase Tip60. Science 293:115-120.

Catala I, Ferrer I, Galofre E, Fabregues I (1988) Decreased numbers of dendritic spines on cortical pyramidal neurons in dementia. A quantitative Golgi study on biopsy samples. Hum Neurobiol 6:255-259.

Chan SL, Culmsee C, Haughey N, Klapper W, Mattson MP (2002) Presenilin-1 mutations sensitize neurons to DNA damage-induced death by a mechanism involving perturbed calcium homeostasis and activation of calpains and caspase-12. Neurobiol Dis 11:2-19.

Chen G, Chen KS, Knox J, Inglis J, Bernard A, Martin SJ, Justice A, McConlogue L, Games D, Freedman SB, Morris RG (2000) A learning deficit related to age and beta-amyloid plaques in a mouse model of Alzheimer's disease. Nature 408:975-979.

Chishti MA, Yang DS, Janus C, Phinney AL, Horne P, Pearson J, Strome R, Zuker N, Loukides J, French J, Turner S, Lozza G, Grilli M, Kunicki S, Morissette C, Paquette J, Gervais F, Bergeron C, Fraser PE, Carlson GA, George-Hyslop PS, Westaway D (2001) Early-onset amyloid deposition and cognitive deficits in transgenic mice expressing a double mutant form of amyloid precursor protein 695. J Biol Chem 276:21562-21570.

Clarke R, Smith AD, Jobst KA, Refsum H, Sutton L, Ueland PM (1998) Folate, vitamin B12, and serum total homocysteine levels in confirmed Alzheimer disease. Arch Neurol 55:1449-1455.

Cleary JP, Walsh DM, Hofmeister JJ, Shankar GM, Kuskowski MA, Selkoe DJ, Ashe KH (2005) Natural oligomers of the amyloid-beta protein specifically disrupt cognitive function. Nat Neurosci 8:79-84.

Cobb JL, Wolf PA, Au R, White R, D'Agostino RB (1995) The effect of education on the incidence of dementia and Alzheimer's disease in the Framingham Study. Neurology 45:1707-1712.

Conti F, Fabri M, Manzoni T (1988) Glutamate-positive corticocortical neurons in the somatic sensory areas I and II of cats. J Neurosci 8:2948-2960.

Corder EH, Saunders AM, Strittmatter WJ, Schmechel DE, Gaskell PC, Small GW, Roses AD, Haines JL, Pericak-Vance MA (1993) Gene dose of apolipoprotein E type 4 allele and the risk of Alzheimer's disease in late onset families. Science 261:921-923.

Cupers P, Orlans I, Craessaerts K, Annaert W, De Strooper B (2001) The amyloid precursor protein (APP)-cytoplasmic fragment generated by gamma-secretase is rapidly degraded but distributes partially in a nuclear fraction of neurones in culture. J Neurochem 78:1168-1178.

Davidoff LM (1928) The brain in mongolian idiocy: report of 10 cases. Archives of neurology and psychiatry 20:1229-1257.

de Ruiter JP, Uylings HB (1987) Morphometric and dendritic analysis of fascia dentata granule cells in human aging and senile dementia. Brain Res 402:217-229.

DeKosky ST, Scheff SW, Styren SD (1996) Structural correlates of cognition in dementia: quantification and assessment of synapse change. Neurodegeneration 5:417-421.

Delaere P, Duyckaerts C, Masters C, Beyreuther K, Piette F, Hauw JJ (1990) Large amounts of neocortical beta A4 deposits without neuritic plaques nor tangles in a psychometrically assessed, non-demented person. Neurosci Lett 116:87-93.

Deller T, Jucker M (2001) Axonsrossung im Zentralnervensystem nach einer Läsion. Neuroforum:11-20.

Dickson DW (1997) The pathogenesis of senile plaques. J Neuropathol Exp Neurol 56:321-339.

Dodart JC, Meziane H, Mathis C, Bales KR, Paul SM, Ungerer A (1999) Behavioral disturbances in transgenic mice overexpressing the V717F beta-amyloid precursor protein. Behav Neurosci 113:982-990.

Duyckaerts C, Dickson DW (2003) Neuropathology of Alzheimer's disease. In: Neurodegeneration: The molecular pathology of dementia and movement disorders (Dickson D, ed), pp 47-65. Basel: ISN Neuropath Press.

Dyrks T, Weidemann A, Multhaup G, Salbaum JM, Lemaire HG, Kang J, Muller-Hill B, Masters CL, Beyreuther K (1988) Identification, transmembrane orientation and biogenesis of the amyloid A4 precursor of Alzheimer's disease. Embo J 7:949-957.

Eckman EA, Reed DK, Eckman CB (2001) Degradation of the Alzheimer's amyloid beta peptide by endothelin-converting enzyme. J Biol Chem 276:24540-24548.

Elias MF, Wolf PA, D'Agostino RB, Cobb J, White LR (1993) Untreated blood pressure level is inversely related to cognitive functioning: the Framingham Study. Am J Epidemiol 138:353-364.

Esiri MM, Hyman BT, Beyreuther K, Masters CL (1997) Ageing and Dementia. In: Greenfields Neuropathology 6th Edition, 6. Edition (Graham DI, Lantos PL, eds), pp 153-233. London: Arnold.

Ferri CP, Prince M, Brayne C, Brodaty H, Fratiglioni L, Ganguli M, Hall K, Hasegawa K, Hendrie H, Huang Y, Jorm A, Mathers C, Menezes PR, Rimmer E, Scazufca M (2005) Global prevalence of dementia: a Delphi consensus study. Lancet 366:2112-2117.

Friedland RP (1993) Epidemiology, education, and the ecology of Alzheimer's disease. Neurology 43:246-249.

Fritzsch B, Farinas I, Reichardt LF (1997) Lack of neurotrophin 3 causes losses of both classes of spiral ganglion neurons in the cochlea in a region-specific fashion. J Neurosci 17:6213-6225.

Galuske RA, Singer W (1996) The origin and topography of long-range intrinsic projections in cat visual cortex: a developmental study. Cereb Cortex 6:417-430.

Galuske RA, Schlote W, Bratzke H, Singer W (2000) Interhemispheric asymmetries of the modular structure in human temporal cortex. Science 289:1946-1949.

Games D, Adams D, Alessandrini R, Barbour R, Berthelette P, Blackwell C, Carr T, Clemens J, Donaldson T, Gillespie F, et al. (1995) Alzheimer-type neuropathology in transgenic mice overexpressing V717F beta-amyloid precursor protein. Nature 373:523-527.

Giuffrida R, Rustioni A (1989) Glutamate and aspartate immunoreactivity in cortico-cortical neurons of the sensorimotor cortex of rats. Exp Brain Res 74:41-46.

Glenner GG, Wong CW (1984) Alzheimer's disease: initial report of the purification and characterization of a novel cerebrovascular amyloid protein. Biochem Biophys Res Commun 120:885-890.

Godement P, Vanselow J, Thanos S, Bonhoeffer F (1987) A study in developing visual systems with a new method of staining neurones and their processes in fixed tissue. Development 101:697-713.

Gowing E, Roher AE, Woods AS, Cotter RJ, Chaney M, Little SP, Ball MJ (1994) Chemical characterization of A beta 17-42 peptide, a component of diffuse amyloid deposits of Alzheimer disease. J Biol Chem 269:10987-10990.

Griffin WS, Sheng JG, Roberts GW, Mrak RE (1995) Interleukin-1 expression in different plaque types in Alzheimer's disease: significance in plaque evolution. J Neuropathol Exp Neurol 54:276-281.

Griffin WS, Stanley LC, Ling C, White L, MacLeod V, Perrot LJ, White CL, 3rd, Araoz C (1989) Brain interleukin 1 and S-100 immunoreactivity are elevated in Down syndrome and Alzheimer disease. Proc Natl Acad Sci U S A 86:7611-7615.

Grober E, Kawas C (1997) Learning and retention in preclinical and early Alzheimer's disease. Psychol Aging 12:183-188.

Grundke-Iqbal I, Iqbal K, Tung YC, Quinlan M, Wisniewski HM, Binder LI (1986) Abnormal phosphorylation of the microtubule-associated protein tau (tau) in Alzheimer cytoskeletal pathology. Proc Natl Acad Sci U S A 83:4913-4917.

Haass C, Schlossmacher MG, Hung AY, Vigo-Pelfrey C, Mellon A, Ostaszewski BL, Lieberburg I, Koo EH, Schenk D, Teplow DB, et al. (1992) Amyloid beta-peptide is produced by cultured cells during normal metabolism. Nature 359:322-325.

Hampel H, Teipel SJ, Alexander GE, Horwitz B, Teichberg D, Schapiro MB, Rapoport SI (1998) Corpus callosum atrophy is a possible indicator of region- and cell type-specific neuronal degeneration in Alzheimer disease: a magnetic resonance imaging analysis. Arch Neurol 55:193-198.

Hardy J (1990) Molecular genetics of Alzheimer's disease. Acta Neurol Scand Suppl 129:29-31.

Hardy J (1997) Amyloid, the presenilins and Alzheimer's disease. Trends Neurosci 20:154-159.

Hardy JA, Goate AM, Owen MJ, Mullan MJ, Rossor MN, Pearson RC (1989) Modelling the occurrence and pathology of Alzheimer's disease. Neurobiol Aging 10:429-431; discussion 446-428.

Hashimoto T, Wakabayashi T, Watanabe A, Kowa H, Hosoda R, Nakamura A, Kanazawa I, Arai T, Takio K, Mann DM, Iwatsubo T (2002) CLAC: a novel Alzheimer amyloid plaque component derived from a transmembrane precursor, CLAC-P/collagen type XXV. Embo J 21:1524-1534.

Haughey NJ, Nath A, Chan SL, Borchard AC, Rao MS, Mattson MP (2002) Disruption of neurogenesis by amyloid beta-peptide, and perturbed neural progenitor cell homeostasis, in models of Alzheimer's disease. J Neurochem 83:1509-1524.

Haugland R (2005) The Handbook: A Guide to Fluorescence Probes and Labeling Technologies. U.S.A: Molecular Probes, Invitrogen detection technologies.

Herzig MC, Winkler DT, Burgermeister P, Pfeifer M, Kohler E, Schmidt SD, Danner S, Abramowski D, Sturchler-Pierrat C, Burki K, van Duinen SG, Maat-Schieman ML, Staufenbiel M, Mathews PM, Jucker M (2004) Abeta is targeted to the vasculature in a mouse model of hereditary cerebral hemorrhage with amyloidosis. Nat Neurosci 7:954-960.

Heston LL, Mastri AR, Anderson VE, White J (1981) Dementia of the Alzheimer type. Clinical genetics, natural history, and associated conditions. Arch Gen Psychiatry 38:1085-1090.

Hofman A, Ott A, Breteler MM, Bots ML, Slooter AJ, van Harskamp F, van Duijn CN, Van Broeckhoven C, Grobbee DE (1997) Atherosclerosis, apolipoprotein E, and prevalence of dementia and Alzheimer's disease in the Rotterdam Study. Lancet 349:151-154.

Honig MG, Hume RI (1986) Fluorescent carbocyanine dyes allow living neurons of identified origin to be studied in long-term cultures. J Cell Biol 103:171-187.

Honig MG, Hume RI (1989) Dil and diO: versatile fluorescent dyes for neuronal labelling and pathway tracing. Trends Neurosci 12:333-335, 340-331.

Hsiao K, Chapman P, Nilsen S, Eckman C, Harigaya Y, Younkin S, Yang F, Cole G (1996) Correlative memory deficits, Abeta elevation, and amyloid plaques in transgenic mice. Science 274:99-102.

Hsu SM, Raine L, Fanger H (1981) Use of avidin-biotin-peroxidase complex (ABC) in immunoperoxidase techniques: a comparison between ABC and unlabeled antibody (PAP) procedures. J Histochem Cytochem 29:577-580.

Hughes CM, Peters A (1992) Types of callosally projecting nonpyramidal neurons in rat visual cortex identified by lysosomal HRP retrograde labeling. Anat Embryol (Berl) 186:183-193.

Irizarry MC, Soriano F, McNamara M, Page KJ, Schenk D, Games D, Hyman BT (1997) Abeta deposition is associated with neuropil changes, but not with overt neuronal loss in the human amyloid precursor protein V717F (PDAPP) transgenic mouse. J Neurosci 17:7053-7059.

Iwata N, Tsubuki S, Takaki Y, Watanabe K, Sekiguchi M, Hosoki E, Kawashima-Morishima M, Lee HJ, Hama E, Sekine-Aizawa Y, Saido TC (2000) Identification of the major Abeta1-42-degrading catabolic pathway in brain parenchyma: suppression leads to biochemical and pathological deposition. Nat Med 6:143-150.

Iwatsubo T, Odaka A, Suzuki N, Mizusawa H, Nukina N, Ihara Y (1994) Visualization of A beta 42(43) and A beta 40 in senile plaques with end-specific A beta monoclonals: evidence that an initially deposited species is A beta 42(43). Neuron 13:45-53.

Janus C, Pearson J, McLaurin J, Mathews PM, Jiang Y, Schmidt SD, Chishti MA, Horne P, Heslin D, French J, Mount HT, Nixon RA, Mercken M, Bergeron C, Fraser PE, St George-Hyslop P, Westaway D (2000) A beta peptide immunization reduces behavioural impairment and plaques in a model of Alzheimer's disease. Nature 408:979-982.

Kalmijn S, Launer LJ, Lindemans J, Bots ML, Hofman A, Breteler MM (1999) Total homocysteine and cognitive decline in a community-based sample of elderly subjects: the Rotterdam Study. Am J Epidemiol 150:283-289.

Kalus P, Braak H, Braak E, Bohl J (1989) The presubicular region in Alzheimer's disease: topography of amyloid deposits and neurofibrillary changes. Brain Res 494:198-203.

Kang J, Lemaire HG, Unterbeck A, Salbaum JM, Masters CL, Grzeschik KH, Multhaup G, Beyreuther K, Muller-Hill B (1987) The precursor of Alzheimer's disease amyloid A4 protein resembles a cell-surface receptor. Nature 325:733-736.

Katzman R (1993) Education and the prevalence of dementia and Alzheimer's disease. Neurology 43:13-20.

Kayed R, Head E, Thompson JL, McIntire TM, Milton SC, Cotman CW, Glabe CG (2003) Common structure of soluble amyloid oligomers implies common mechanism of pathogenesis. Science 300:486-489.

Kelly PH, Bondolfi L, Hunziker D, Schlecht HP, Carver K, Maguire E, Abramowski D, Wiederhold KH, Sturchler-Pierrat C, Jucker M, Bergmann R, Staufenbiel M, Sommer B (2003) Progressive age-related impairment of cognitive behavior in APP23 transgenic mice. Neurobiol Aging 24:365-378.

Kim HJ, Chae SC, Lee DK, Chromy B, Lee SC, Park YC, Klein WL, Krafft GA, Hong ST (2003) Selective neuronal degeneration induced by soluble oligomeric amyloid beta protein. Faseb J 17:118-120.

Kimberly WT, Zheng JB, Guenette SY, Selkoe DJ (2001) The intracellular domain of the beta-amyloid precursor protein is stabilized by Fe65 and translocates to the nucleus in a notch-like manner. J Biol Chem 276:40288-40292.

Kitaguchi N, Takahashi Y, Tokushima Y, Shiojiri S, Ito H (1988) Novel precursor of Alzheimer's disease amyloid protein shows protease inhibitory activity. Nature 331:530-532.

Klafki HW, Wiltfang J, Staufenbiel M (1996) Electrophoretic separation of betaA4 peptides (1-40) and (1-42). Anal Biochem 237:24-29.

Knopman D (2003) Alzheimer Type Dementia. In: Neurodegeneration: The molecular pathology of dementia and movement disorders (Dickson D, ed), pp 24-39. Basel: ISN Neuropath Press.

Knopman DS, Ryberg S (1989) A verbal memory test with high predictive accuracy for dementia of the Alzheimer type. Arch Neurol 46:141-145.

Knyihar-Csillik E, Csillik B, Oestreicher AB (1992) Light and electron microscopic localization of B-50 (GAP43) in the rat spinal cord during transganglionic degenerative atrophy and regeneration. J Neurosci Res 32:93-109.

Koistinaho M, Lin S, Wu X, Esterman M, Koger D, Hanson J, Higgs R, Liu F, Malkani S, Bales KR, Paul SM (2004) Apolipoprotein E promotes astrocyte colocalization and degradation of deposited amyloid-beta peptides. Nat Med 10:719-726.

Kokubo H, Kayed R, Glabe CG, Yamaguchi H (2005a) Soluble Abeta oligomers ultrastructurally localize to cell processes and might be related to synaptic dysfunction in Alzheimer's disease brain. Brain Res 1031:222-228.

Kokubo H, Kayed R, Glabe CG, Saido TC, Iwata N, Helms JB, Yamaguchi H (2005b) Oligomeric proteins ultrastructurally localize to cell processes, especially to axon terminals with higher density, but not to lipid rafts in Tg2576 mouse brain. Brain Res 1045:224-228.

Kosik KS, Joachim CL, Selkoe DJ (1986) Microtubule-associated protein tau (tau) is a major antigenic component of paired helical filaments in Alzheimer disease. Proc Natl Acad Sci U S A 83:4044-4048.

Lacor PN, Buniel MC, Klein WL (2004) ADDLs (Abeta oligomers) alter structure and function of synaptic spines. 2004 Abstract Viewer/Itinerary Planner:Program No. 218.213.

Lamy C, Duyckaerts C, Delaere P, Payan C, Fermanian J, Poulain V, Hauw JJ (1989) Comparison of seven staining methods for senile plaques and neurofibrillary tangles in a prospective series of 15 elderly patients. Neuropathol Appl Neurobiol 15:563-578.

Lautenschlager NT, Cupples LA, Rao VS, Auerbach SA, Becker R, Burke J, Chui H, Duara R, Foley EJ, Glatt SL, Green RC, Jones R, Karlinsky H, Kukull WA, Kurz A, Larson EB, Martelli K, Sadovnick AD, Volicer L, Waring SC, Growdon JH, Farrer LA (1996) Risk of dementia among relatives of Alzheimer's disease patients in the MIRAGE study: What is in store for the oldest old? Neurology 46:641-650.

Lesne S, Koh MT, Kotilinek L, Kayed R, Glabe CG, Yang A, Gallagher M, Ashe KH (2006) A specific amyloid-beta protein assembly in the brain impairs memory. Nature 440:352-357.

Lewis J, Dickson DW, Lin WL, Chisholm L, Corral A, Jones G, Yen SH, Sahara N, Skipper L, Yager D, Eckman C, Hardy J, Hutton M, McGowan E (2001) Enhanced neurofibrillary degeneration in transgenic mice expressing mutant tau and APP. Science 293:1487-1491.

Lord A, Kalimo H, Eckman C, Zhang XQ, Lannfelt L, Nilsson LN (2006) The Arctic Alzheimer mutation facilitates early intraneuronal Abeta aggregation and senile plaque formation in transgenic mice. Neurobiol Aging 27:67-77.

Mandelkow EM, Mandelkow E (1998) Tau in Alzheimer's disease. Trends Cell Biol 8:425-427.

Martinez-Garcia F, Gonzalez-Hernandez T, Martinez-Millan L (1994) Pyramidal and nonpyramidal callosal cells in the striate cortex of the adult rat. J Comp Neurol 350:439-451.

Masliah E, Mallory M, Ge N, Saitoh T (1992a) Amyloid precursor protein is localized in growing neurites of neonatal rat brain. Brain Res 593:323-328.

Masliah E, Sisk A, Mallory M, Games D (2001) Neurofibrillary pathology in transgenic mice overexpressing V717F beta-amyloid precursor protein. J Neuropathol Exp Neurol 60:357-368.

Masliah E, Mallory M, Hansen L, Alford M, DeTeresa R, Terry R, Baudier J, Saitoh T (1992b) Localization of amyloid precursor protein in GAP43-immunoreactive aberrant sprouting neurites in Alzheimer's disease. Brain Res 574:312-316.

Masters CL, Beyreuther K (2003) Molecular Pathogenesis of Alzheimer's disease. In: Neurodegeneration: The Molecular Pathology of Dementia and Movement Disorders (Dickson D, ed), pp 69-73. Basel: ISN Neuropath Press.

Masters CL, Multhaup G, Simms G, Pottgiesser J, Martins RN, Beyreuther K (1985a) Neuronal origin of a cerebral amyloid: neurofibrillary tangles of Alzheimer's disease contain the same protein as the amyloid of plaque cores and blood vessels. Embo J 4:2757-2763.

Masters CL, Simms G, Weinman NA, Multhaup G, McDonald BL, Beyreuther K (1985b) Amyloid plaque core protein in Alzheimer disease and Down syndrome. Proc Natl Acad Sci U S A 82:4245-4249.

Mattson MP (2000) Apoptosis in neurodegenerative disorders. Nat Rev Mol Cell Biol 1:120-129.

Mayeux R, Ottman R, Maestre G, Ngai C, Tang MX, Ginsberg H, Chun M, Tycko B, Shelanski M (1995) Synergistic effects of traumatic head injury and apolipoprotein-epsilon 4 in patients with Alzheimer's disease. Neurology 45:555-557.

McCaddon A, Davies G, Hudson P, Tandy S, Cattell H (1998) Total serum homocysteine in senile dementia of Alzheimer type. Int J Geriatr Psychiatry 13:235-239.

McGeer PL, Akiyama H, Itagaki S, McGeer EG (1989) Activation of the classical complement pathway in brain tissue of Alzheimer patients. Neurosci Lett 107:341-346.

McGowan E, Pickford F, Kim J, Onstead L, Eriksen J, Yu C, Skipper L, Murphy MP, Beard J, Das P, Jansen K, Delucia M, Lin WL, Dolios G, Wang R, Eckman CB, Dickson DW, Hutton M, Hardy J, Golde T (2005) Abeta42 is essential for parenchymal and vascular amyloid deposition in mice. Neuron 47:191-199.

Miller BC, Eckman EA, Sambamurti K, Dobbs N, Chow KM, Eckman CB, Hersh LB, Thiele DL (2003) Amyloid-beta peptide levels in brain are inversely correlated with insulysin activity levels in vivo. Proc Natl Acad Sci U S A 100:6221-6226.

Moechars D, Dewachter I, Lorent K, Reverse D, Baekelandt V, Naidu A, Tesseur I, Spittaels K, Haute CV, Checler F, Godaux E, Cordell B, Van Leuven F (1999) Early phenotypic changes in transgenic mice that overexpress different mutants of amyloid precursor protein in brain. J Biol Chem 274:6483-6492.

Morgan D, Diamond DM, Gottschall PE, Ugen KE, Dickey C, Hardy J, Duff K, Jantzen P, DiCarlo G, Wilcock D, Connor K, Hatcher J, Hope C, Gordon M, Arendash GW (2000) A beta peptide vaccination prevents memory loss in an animal model of Alzheimer's disease. Nature 408:982-985.

Morimoto A, Irie K, Murakami K, Masuda Y, Ohigashi H, Nagao M, Fukuda H, Shimizu T, Shirasawa T (2004) Analysis of the secondary structure of beta-amyloid (Abeta42) fibrils by systematic proline replacement. J Biol Chem 279:52781-52788.

Morrison JH, Hof PR (1997) Life and death of neurons in the aging brain. Science 278:412-419.

Mouton PR, Martin LJ, Calhoun ME, Dal Forno G, Price DL (1998) Cognitive decline strongly correlates with cortical atrophy in Alzheimer's dementia. Neurobiol Aging 19:371-377.

Mucke L, Masliah E, Yu GQ, Mallory M, Rockenstein EM, Tatsuno G, Hu K, Kholodenko D, Johnson-Wood K, McConlogue L (2000) High-level neuronal expression of abeta 1-42 in wild-

type human amyloid protein precursor transgenic mice: synaptotoxicity without plaque formation. J Neurosci 20:4050-4058.

Namba Y, Tomonaga M, Kawasaki H, Otomo E, Ikeda K (1991) Apolipoprotein E immunoreactivity in cerebral amyloid deposits and neurofibrillary tangles in Alzheimer's disease and kuru plaque amyloid in Creutzfeldt-Jakob disease. Brain Res 541:163-166.

National Institute on Aging, and Reagan Institute Working Group on Diagnostic Criteria for the Neuropathological Assessment of Alzheimer's Disease (1997) Consensus recommendations for the postmortem diagnosis of Alzheimer's disease. Neurobiol Aging 18:S1-2.

Neve RL, Finch EA, Dawes LR (1988) Expression of the Alzheimer amyloid precursor gene transcripts in the human brain. Neuron 1:669-677.

Nicoll JA, Wilkinson D, Holmes C, Steart P, Markham H, Weller RO (2003) Neuropathology of human Alzheimer disease after immunization with amyloid-beta peptide: a case report. Nat Med 9:448-452.

Nilsberth C, Westlind-Danielsson A, Eckman CB, Condron MM, Axelman K, Forsell C, Stenh C, Luthman J, Teplow DB, Younkin SG, Naslund J, Lannfelt L (2001) The 'Arctic' APP mutation (E693G) causes Alzheimer's disease by enhanced Abeta protofibril formation. Nat Neurosci 4:887-893.

Oddo S, Caccamo A, Kitazawa M, Tseng BP, LaFerla FM (2003a) Amyloid deposition precedes tangle formation in a triple transgenic model of Alzheimer's disease. Neurobiol Aging 24:1063-1070.

Oddo S, Caccamo A, Shepherd JD, Murphy MP, Golde TE, Kayed R, Metherate R, Mattson MP, Akbari Y, LaFerla FM (2003b) Triple-transgenic model of Alzheimer's disease with plaques and tangles: intracellular Abeta and synaptic dysfunction. Neuron 39:409-421.

Olichney JM, Hansen LA, Hofstetter CR, Lee JH, Katzman R, Thal LJ (2000) Association between severe cerebral amyloid angiopathy and cerebrovascular lesions in Alzheimer disease is not a spurious one attributable to apolipoprotein E4. Arch Neurol 57:869-874.

Ott A, Breteler MM, van Harskamp F, Claus JJ, van der Cammen TJ, Grobbee DE, Hofman A (1995) Prevalence of Alzheimer's disease and vascular dementia: association with education. The Rotterdam study. Bmj 310:970-973.

Petersen RC, Smith GE, Ivnik RJ, Kokmen E, Tangalos EG (1994) Memory function in very early Alzheimer's disease. Neurology 44:867-872.

Phinney AL, Deller T, Stalder M, Calhoun ME, Frotscher M, Sommer B, Staufenbiel M, Jucker M (1999) Cerebral amyloid induces aberrant axonal sprouting and ectopic terminal formation in amyloid precursor protein transgenic mice. J Neurosci 19:8552-8559.

Pike CJ, Walencewicz AJ, Glabe CG, Cotman CW (1991) In vitro aging of beta-amyloid protein causes peptide aggregation and neurotoxicity. Brain Res 563:311-314.

Podlisny MB, Ostaszewski BL, Squazzo SL, Koo EH, Rydell RE, Teplow DB, Selkoe DJ (1995) Aggregation of secreted amyloid beta-protein into sodium dodecyl sulfate-stable oligomers in cell culture. J Biol Chem 270:9564-9570.

Ponte P, Gonzalez-DeWhitt P, Schilling J, Miller J, Hsu D, Greenberg B, Davis K, Wallace W, Lieberburg I, Fuller F (1988) A new A4 amyloid mRNA contains a domain homologous to serine proteinase inhibitors. Nature 331:525-527.

Price JL, Davis PB, Morris JC, White DL (1991) The distribution of tangles, plaques and related immunohistochemical markers in healthy aging and Alzheimer's disease. Neurobiol Aging 12:295-312.

Rebeck GW, Reiter JS, Strickland DK, Hyman BT (1993) Apolipoprotein E in sporadic Alzheimer's disease: allelic variation and receptor interactions. Neuron 11:575-580.

Reiner A, Veenman CL, Medina L, Jiao Y, Del Mar N, Honig MG (2000) Pathway tracing using biotinylated dextran amines. J Neurosci Methods 103:23-37.

Roos RA, Haan J, Van Broeckhoven C (1991) Hereditary cerebral hemorrhage with amyloidosis--Dutch type: a congophilic angiopathy. An overview. Ann N Y Acad Sci 640:155-160.

Roselli F, Tirard M, Lu J, Hutzler P, Lamberti P, Livrea P, Morabito M, Almeida OF (2005) Soluble beta-amyloid1-40 induces NMDA-dependent degradation of postsynaptic density-95 at glutamatergic synapses. J Neurosci 25:11061-11070.

Saido TC, Yamao-Harigaya W, Iwatsubo T, Kawashima S (1996) Amino- and carboxyl-terminal heterogeneity of beta-amyloid peptides deposited in human brain. Neurosci Lett 215:173-176.

Saido TC, Iwatsubo T, Mann DM, Shimada H, Ihara Y, Kawashima S (1995) Dominant and differential deposition of distinct beta-amyloid peptide species, A beta N3(pE), in senile plaques. Neuron 14:457-466.

Sassin I, Schultz C, Thal DR, Rub U, Arai K, Braak E, Braak H (2000) Evolution of Alzheimer's disease-related cytoskeletal changes in the basal nucleus of Meynert. Acta Neuropathol (Berl) 100:259-269.

Scheff SW, DeKosky ST, Price DA (1990) Quantitative assessment of cortical synaptic density in Alzheimer's disease. Neurobiol Aging 11:29-37.

Schenk D, Barbour R, Dunn W, Gordon G, Grajeda H, Guido T, Hu K, Huang J, Johnson-Wood K, Khan K, Kholodenko D, Lee M, Liao Z, Lieberburg I, Motter R, Mutter L, Soriano F, Shopp G, Vasquez N, Vandevert C, Walker S, Wogulis M, Yednock T, Games D, Seubert P (1999) Immunization with amyloid-beta attenuates Alzheimer-disease-like pathology in the PDAPP mouse. Nature 400:173-177.

Schmitz C, Rutten BP, Pielen A, Schafer S, Wirths O, Tremp G, Czech C, Blanchard V, Multhaup G, Rezaie P, Korr H, Steinbusch HW, Pradier L, Bayer TA (2004) Hippocampal neuron loss

exceeds amyloid plaque load in a transgenic mouse model of Alzheimer's disease. Am J Pathol 164:1495-1502.

Scholz W (1938) Studien zur Pathologie der Hirngefäße. II. Die drusige Entartung der Hirnarterien und -capillaren. (Eine Form seniler Gefäßerkrankung). Z ges Neurol Psychiatr 4:694-715.

Schrader-Fischer G, Paganetti PA (1996) Effect of alkalizing agents on the processing of the beta-amyloid precursor protein. Brain Res 716:91-100.

Seshadri S, Beiser A, Selhub J, Jacques PF, Rosenberg IH, D'Agostino RB, Wilson PW, Wolf PA (2002) Plasma homocysteine as a risk factor for dementia and Alzheimer's disease. N Engl J Med 346:476-483.

Spires TL, Meyer-Luehmann M, Stern EA, McLean PJ, Skoch J, Nguyen PT, Bacskai BJ, Hyman BT (2005) Dendritic spine abnormalities in amyloid precursor protein transgenic mice demonstrated by gene transfer and intravital multiphoton microscopy. J Neurosci 25:7278-7287.

Stadelmann C, Deckwerth TL, Srinivasan A, Bancher C, Bruck W, Jellinger K, Lassmann H (1999) Activation of caspase-3 in single neurons and autophagic granules of granulovacuolar degeneration in Alzheimer's disease. Evidence for apoptotic cell death. Am J Pathol 155:1459-1466.

Staufenbiel M, Paganetti PA (1999) Electrophoretic Separation and Immunoblotting of Aβ1-40 and Aβ1-42. In: Methods in Molecular Medicine: Alzheimer's Disease: Methods and Protocols. Totowa, NJ: Humana Press Inc.

Stern RG, Mohs RC, Davidson M, Schmeidler J, Silverman J, Kramer-Ginsberg E, Searcey T, Bierer L, Davis KL (1994) A longitudinal study of Alzheimer's disease: measurement, rate, and predictors of cognitive deterioration. Am J Psychiatry 151:390-396.

Stern Y, Tang MX, Denaro J, Mayeux R (1995) Increased risk of mortality in Alzheimer's disease patients with more advanced educational and occupational attainment. Ann Neurol 37:590-595.

Storandt M, Botwinick J, Danziger WL, Berg L, Hughes CP (1984) Psychometric differentiation of mild senile dementia of the Alzheimer type. Arch Neurol 41:497-499.

Strauss S, Bauer J, Ganter U, Jonas U, Berger M, Volk B (1992) Detection of interleukin-6 and alpha 2-macroglobulin immunoreactivity in cortex and hippocampus of Alzheimer's disease patients. Lab Invest 66:223-230.

Sturchler-Pierrat C, Abramowski D, Duke M, Wiederhold KH, Mistl C, Rothacher S, Ledermann B, Burki K, Frey P, Paganetti PA, Waridel C, Calhoun ME, Jucker M, Probst A, Staufenbiel M, Sommer B (1997) Two amyloid precursor protein transgenic mouse models with Alzheimer disease-like pathology. Proc Natl Acad Sci U S A 94:13287-13292.

Takahashi RH, Almeida CG, Kearney PF, Yu F, Lin MT, Milner TA, Gouras GK (2004) Oligomerization of Alzheimer's beta-amyloid within processes and synapses of cultured neurons and brain. J Neurosci 24:3592-3599.

Tanzi RE, McClatchey AI, Lamperti ED, Villa-Komaroff L, Gusella JF, Neve RL (1988) Protease inhibitor domain encoded by an amyloid protein precursor mRNA associated with Alzheimer's disease. Nature 331:528-530.

Terry RD, DeTeresa R, Hansen LA (1987) Neocortical cell counts in normal human adult aging. Ann Neurol 21:530-539.

Terry RD, Peck A, DeTeresa R, Schechter R, Horoupian DS (1981) Some morphometric aspects of the brain in senile dementia of the Alzheimer type. Ann Neurol 10:184-192.

Teter B, Ashford JW (2002) Neuroplasticity in Alzheimer's disease. J Neurosci Res 70:402-437.

Thal DR, Schober R, Birkenmeier G (1997) The subunits of alpha2-macroglobulin receptor/low density lipoprotein receptor-related protein, native and transformed alpha2-macroglobulin and interleukin 6 in Alzheimer's disease. Brain Res 777:223-227.

Thal DR, Del Tredici K, Braak H (2004) Neurodegeneration in Normal Brain Aging and Disease. Sci Aging Knowledge Environ in press.

Thal DR, Rüb U, Orantes M, Braak H (2002a) Phases of Abeta-deposition in the human brain and its relevance for the development of AD. Neurology 58:1791-1800.

Thal DR, Ghebremedhin E, Haass C, Schultz C (2002b) UV light-induced autofluorescence of full-length Abeta-protein deposits in the human brain. Clin Neuropathol 21:35-40.

Thal DR, Capetillo-Zarate E, Del Tredici K, Braak H (2006a) The development of amyloid β-protein (Aβ)-deposits in the aged brain. Sci Aging Knowl Environ.

Thal DR, Sassin I, Schultz C, Haass C, Braak E, Braak H (1999) Fleecy amyloid deposits in the internal layers of the human entorhinal cortex are comprised of N-terminal truncated fragments of Abeta. J Neuropathol Exp Neurol 58:210-216.

Thal DR, Ghebremedhin E, Rüb U, Yamaguchi H, Del Tredici K, Braak H (2002c) Two types of sporadic cerebral amyloid angiopathy. J Neuropathol Exp Neurol 61:282-293.

Thal DR, Holzer M, Rüb U, Waldmann G, Gunzel S, Zedlick D, Schober R (2000a) Alzheimer-related tau-pathology in the perforant path target zone and in the hippocampal stratum oriens and radiatum correlates with onset and degree of dementia. Exp Neurol 163:98-110.

Thal DR, Rüb U, Schultz C, Sassin I, Ghebremedhin E, Del Tredici K, Braak E, Braak H (2000b) Sequence of Abeta-protein deposition in the human medial temporal lobe. J Neuropathol Exp Neurol 59:733-748.

Thal DR, Larionov S, Abramowski D, Wiederhold KH, Van Dooren T, Yamaguchi H, Haass C, Van Leuven F, Staufenbiel M, Capetillo-Zarate E (2006b) Occurrence and co-localization of amyloid beta-protein and apolipoprotein E in perivascular drainage channels of wild-type and APP-transgenic mice. Neurobiol Aging.

Thal DR, Capetillo-Zarate E, Schultz C, Rub U, Saido TC, Yamaguchi H, Haass C, Griffin WS, Del Tredici K, Braak H, Ghebremedhin E (2005) Apolipoprotein E co-localizes with newly formed amyloid beta-protein (Abeta) deposits lacking immunoreactivity against N-terminal epitopes of Abeta in a genotype-dependent manner. Acta Neuropathol (Berl) 110:459-471.

Tomidokoro Y, Harigaya Y, Matsubara E, Ikeda M, Kawarabayashi T, Shirao T, Ishiguro K, Okamoto K, Younkin SG, Shoji M (2001a) Brain Abeta amyloidosis in APPsw mice induces accumulation of presenilin-1 and tau. J Pathol 194:500-506.

Tomidokoro Y, Ishiguro K, Harigaya Y, Matsubara E, Ikeda M, Park JM, Yasutake K, Kawarabayashi T, Okamoto K, Shoji M (2001b) Abeta amyloidosis induces the initial stage of tau accumulation in APP(Sw) mice. Neurosci Lett 299:169-172.

Tsai J, Grutzendler J, Duff K, Gan WB (2004) Fibrillar amyloid deposition leads to local synaptic abnormalities and breakage of neuronal branches. Nat Neurosci 7:1181-1183.

Van Dam D, D'Hooge R, Staufenbiel M, Van Ginneken C, Van Meir F, De Deyn PP (2003) Age-dependent cognitive decline in the APP23 model precedes amyloid deposition. Eur J Neurosci 17:388-396.

Vassar R, Bennett BD, Babu-Khan S, Kahn S, Mendiaz EA, Denis P, Teplow DB, Ross S, Amarante P, Loeloff R, Luo Y, Fisher S, Fuller J, Edenson S, Lile J, Jarosinski MA, Biere AL, Curran E, Burgess T, Louis JC, Collins F, Treanor J, Rogers G, Citron M (1999) Beta-secretase cleavage of Alzheimer's amyloid precursor protein by the transmembrane aspartic protease BACE. Science 286:735-741.

Vetrivel KS, Thinakaran G (2006) Amyloidogenic processing of beta-amyloid precursor protein in intracellular compartments. Neurology 66:S69-73.

Vidal R, Frangione B, Rostagno A, Mead S, Revesz T, Plant G, Ghiso J (1999) A stop-codon mutation in the BRI gene associated with familial British dementia. Nature 399:776-781.

Vinters HV, Gilbert JJ (1983) Cerebral amyloid angiopathy: incidence and complications in the aging brain. II. The distribution of amyloid vascular changes. Stroke 14:924-928.

Virchow R (1854) Zur Cellulose-Frage. Virchows Arch Path Anat 6:416-426.

Virchow R (1855) Veber den Gang der amyloiden Degeneration. Virchows Arch Path Anat 8:364-368.

Voigt T, LeVay S, Stamnes MA (1988) Morphological and immunocytochemical observations on the visual callosal projections in the cat. J Comp Neurol 272:450-460.

Wang D, Munoz DG (1995) Qualitative and quantitative differences in senile plaque dystrophic neurites of Alzheimer's disease and normal aged brain. J Neuropathol Exp Neurol 54:548-556.

Wang HW, Pasternak JF, Kuo H, Ristic H, Lambert MP, Chromy B, Viola KL, Klein WL, Stine WB, Krafft GA, Trommer BL (2002) Soluble oligomers of beta amyloid (1-42) inhibit long-term potentiation but not long-term depression in rat dentate gyrus. Brain Res 924:133-140.

Weidemann A, Konig G, Bunke D, Fischer P, Salbaum JM, Masters CL, Beyreuther K (1989) Identification, biogenesis, and localization of precursors of Alzheimer's disease A4 amyloid protein. Cell 57:115-126.

Weis S, Jellinger K, Wenger E (1991) Morphometry of the corpus callosum in normal aging and Alzheimer's disease. J Neural Transm Suppl 33:35-38.

Weller RO, Massey A, Newman TA, Hutchings M, Kuo YM, Roher AE (1998) Cerebral amyloid angiopathy: amyloid beta accumulates in putative interstitial fluid drainage pathways in Alzheimer's disease. Am J Pathol 153:725-733.

Welsh K, Butters N, Hughes J, Mohs R, Heyman A (1991) Detection of abnormal memory decline in mild cases of Alzheimer's disease using CERAD neuropsychological measures. Arch Neurol 48:278-281.

West MJ (1993) Regionally specific loss of neurons in the aging human hippocampus. Neurobiol Aging 14:287-293.

West MJ, Coleman PD, Flood DG, Troncoso JC (1994) Differences in the pattern of hippocampal neuronal loss in normal ageing and Alzheimer's disease. Lancet 344:769-772.

Wiederhold K-H, Staufenbiel M, Mistl C, Danner S (2004) Stages of amyloid deposition and plaque types in different APP transgenic mice as compared to AD (Abstract). Neurobiology of Aging 25 Suppl. 2:254-255.

Wild-Bode C, Yamazaki T, Capell A, Leimer U, Steiner H, Ihara Y, Haass C (1997) Intracellular generation and accumulation of amyloid beta-peptide terminating at amino acid 42. J Biol Chem 272:16085-16088.

Winkler DT, Bondolfi L, Herzig MC, Jann L, Calhoun ME, Wiederhold KH, Tolnay M, Staufenbiel M, Jucker M (2001) Spontaneous hemorrhagic stroke in a mouse model of cerebral amyloid angiopathy. J Neurosci 21:1619-1627.

Wirths O, Multhaup G, Czech C, Blanchard V, Moussaoui S, Tremp G, Pradier L, Beyreuther K, Bayer TA (2001) Intraneuronal Abeta accumulation precedes plaque formation in beta-amyloid precursor protein and presenilin-1 double-transgenic mice. Neurosci Lett 306:116-120.

Wise SP, Jones EG (1976) The organization and postnatal development of the commissural projection of the rat somatic sensory cortex. J Comp Neurol 168:313-343.

Wisniewski HM, Sadowski M, Jakubowska-Sadowska K, Tarnawski M, Wegiel J (1998) Diffuse, lake-like amyloid-beta deposits in the parvopyramidal layer of the presubiculum in Alzheimer disease. J Neuropathol Exp Neurol 57:674-683.

Wouterlood FG (1993) Neuroscience Protocols: Elservier Science Publisher.

Wu CC, Chawla F, Games D, Rydel RE, Freedman S, Schenk D, Young WG, Morrison JH, Bloom FE (2004) Selective vulnerability of dentate granule cells prior to amyloid deposition in PDAPP mice: digital morphometric analyses. Proc Natl Acad Sci U S A 101:7141-7146.

Yamaguchi H, Sugihara S, Ogawa A, Saido TC, Ihara Y (1998) Diffuse plaques associated with astroglial amyloid beta protein, possibly showing a disappearing stage of senile plaques. Acta Neuropathol (Berl) 95:217-222.

Yamauchi H, Fukuyama H, Harada K, Nabatame H, Ogawa M, Ouchi Y, Kimura J, Konishi J (1993) Callosal atrophy parallels decreased cortical oxygen metabolism and neuropsychological impairment in Alzheimer's disease. Arch Neurol 50:1070-1074.

Zhang MY, Katzman R, Salmon D, Jin H, Cai GJ, Wang ZY, Qu GY, Grant I, Yu E, Levy P, et al. (1990) The prevalence of dementia and Alzheimer's disease in Shanghai, China: impact of age, gender, and education. Ann Neurol 27:428-437.

ACKNOWLEDGMENTS

I would like to express my gratitude to my supervisor, PD. Dr. med. D. R. Thal, for providing me with such an interesting topic, for the excellent supervision and support during this work.

I wish to thank to all colleagues of the Institute of Neuropathology, especially to Prof. Dr. med. O. D. Wiestler and Prof. Dr. med. T. Pietsch for the opportunity to carry out this work in this institute.

I wish to thank Prof. Dr. rer. nat. W. Kolanus, Prof. Dr. rer. nat. K. Willecke and P.D. Dr. rer. nat. G. van Echten-Deckert for the interest and time applied for the assessment of this work.

I wish to thank all my co-authors, D. Abramowski, H. Braak, K. Del Tredici, A. Escher, E. Ghebremedhin, W. S. T. Griffin, C. Haass, S. Larionov, U. Rüb, T. C. Saido, C. Schultz, C. Stadelmann, M. Staufenbiel, T. Van Dooren, F. Van Leuven, K. H. Wiederhold and H. Yamaguchi for the valuable contribution to this work.

I am very grateful to M. Staufenbiel and D. Abramoswski at the Novartis Institutes for Biomedical Research (Basel, Switzerland) for providing the animal models and performing the western blot and ELISA analysis; to C. Stadelmann and A. Escher at the Department of Neuropathology, Georg-August University (Göttingen, Germany) for providing the BDA traced samples; to C. Haass at the Department of Biochemistry, Adolf-Butenandt Institute, Ludwig Maximilians University (Munich, Germany) and H. Yamaguchi at the Gunma University School of Health Sciences (Maebashi, Gunma, Japan) for the kind gift of the antibodies and to H. Braak at the Institute for Clinical Neuroanantomy, J. W. Goethe University (Frankfurt am Main, Germany) for providing some of the diagrams.

I wish to thank Magdalena Sastre and Panagiotis Theofilas for the suggestions to improve the manuscript.

I wish to thank all members of the group, it was a real pleasure to work and share this time with you all, and especially to Uta Enderlein and Nicole Kolosnjaji because without your help this work would not be possible, thanks.

Acknowledgments

I wish also to thank H. U. Klatt for the excellent design and photographic work and to C. Kaschke for the work done with the 3D reconstructions of the DiI traced sections.

During my time in Bonn I have made very good friends from Bulgaria, Greece, Germany, Spain, Tunisia, U.S.A. and other countries, my warmest thank to all of you for you help, support, for been available at any time, for the nice time we had and for the nice time we will have together.

My special thanks to Ana A., Ana S. de O., Gaizka O., Iratxe D, Iratxe L. de A., Maider E. Orella G. de I. and Pablo O., because you are with me wherever I am.

Finally, I will like to dedicate this work to my family because it means as much for them as it means for me. You have taught me that nothing is impossible, and with work, confidence and respect everybody can reach their objectives, thanks for supporting me always.

This study was supported by DFG-grant No. TH624/2 and BONFOR-grants No. O-154.0041, O-154.0068.

Estibaliz Capetillo Gonzalez de Zarate

ERKLÄRUNG/DECLARATION

Hiermit versichere ich, dass diese Dissertation von mir persönlich, selbständig und ohne jede unerlaubte Hilfe angefertigt wurde. Die Daten, die im Rahmen einer Kooperation gewonnen wurden, sind ausnahmslos gekennzeichnet. Die vorliegende Arbeit wurde an keiner anderen Hochschule als Dissertation eingereicht. Ich habe früher noch keinen Promotionsversuch unternommen. Diese Dissertation wurde an der nachstehend aufgeführten Stelle auszugsweise veröffentlicht.

Capetillo-Zarate, E.; Staufenbiel, M.; Abramowski, D.; Haass, C.; Escher, A.; Stadelmann, C.; Yamaguchi, H.; Wiestler, O.D.; Thal, D.R. (2006) Selective vulnerability of different types of commissural neurons for amyloid β-protein induced neurodegeneration in APP23 mice correlates with dendritic tree morphology. *Brain,* published online (DOI: 10.1093/brain/aw1176).

Thal, D.R.; Capetillo-Zarate, E.; Del Tredici, K.; Braak, H. (2006) The development of amyloid β protein (Aβ)-deposits in the aged brain. *Sci. Aging. Knowl. Environ*. Mar 8; (6): re1.

Bonn, 09.11.2006

Estibaliz Capetillo Gonzalez de Zarate

LIST OF PUBLICATIONS

Original articles

Capetillo-Zarate, E.; Staufenbiel, M.; Abramowski, D.; Haass, C.; Escher, A.; Stadelmann, C.; Yamaguchi, H.; Wiestler, O.; Thal, D. (2006) Selective vulnerability of different types of commissural neurons for amyloid β-protein induced neurodegeneration in APP23 mice correlates with dendritic tree morphology. *Brain, in press, published online.*

Thal, D; Larionov, S.; Abramowski, D.; Wiederhold, K. H.; Van Dooren, T.; Yamaguchi, H.; Haass, C.; Van Leuven, F.; Staufenbiel, M.; Capetillo-Zarate, E. (2006) Occurrence and co-localization of amyloid β-protein and apolipoprotein E in perivascular drainage channels of wild-type and APP-transgenic mice. *Neurobiology of Aging, in press, published online.*

Thal, D.R.; Capetillo-Zarate, E.; Schultz, C.; Rüb, U.; Saido, T.C.; Yamaguchi, H.; Haass, C.; Griffin, W.S.T.; Del Tredici, K.; Braak, H.; Ghebremedhin, E. (2005) Apolipoprotein E co-localizes with newly formed amyloid β-protein (Aβ)-deposits lacking immunoreactivity against N-terminal epitopes of Aβ in a genotype-dependent manner. *Acta Neuropathol (Berl).* Nov; 110(5):459-71.

Reviews

Thal, D.R.; Capetillo-Zarate, E.; Del Tredici, K.; Braak, H. (2006) The development of amyloid β-protein (Aβ)-deposits in the aged brain. *Sci. Aging. Knowl. Environ.* Mar 8; (6): re1.